LASER PARTICLE ACCELERATORS IN BRAZIL

PERSPECTIVES FOR A BRAZILIAN PROGRAM

Nilson Dias Vieira Junior
IPEN/CNEN-SP

COMPACT LASER ACCELERATORS FOR MEDICAL APPLICATIONS

- Nilson D. Vieira Jr. - IPEN
- Sudeep Banerjee, University of Nebraska-Lincoln
- Edison P. Maldonado, Instituto Tecnológico de Aeronáutica -ITA
- Armando V. F. Zuffi, - IPEN (Ph. D. student, CNPq)
- Fabio B. D. Tabacow – IPEN (PCI, CNPq)
- Ricardo E. Samad - IPEN

LASER INTENSITIES AND INTERACTIONS

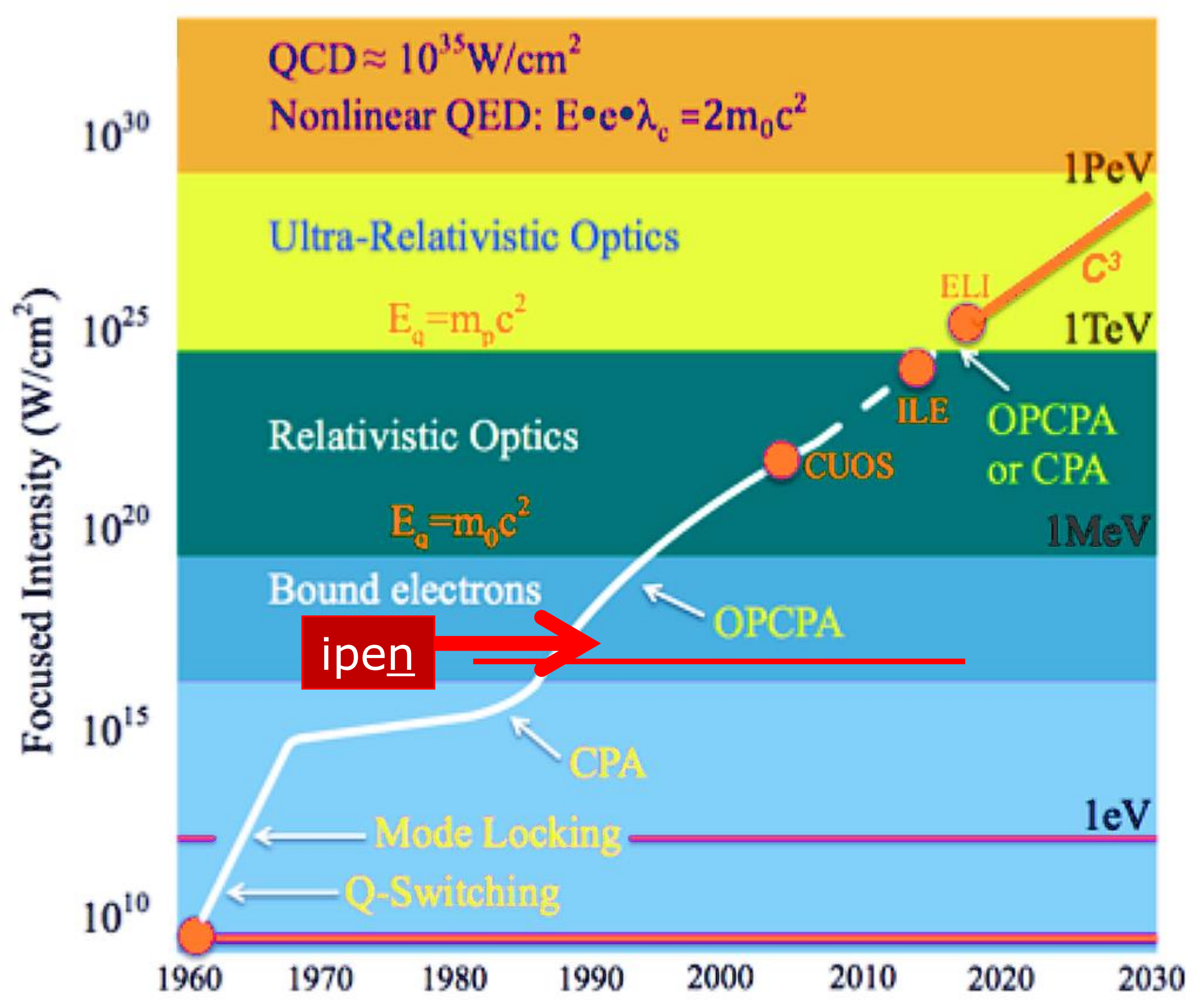

Gerard Mourou, Physics Nobel Prize 2018

CPA: Mourou & Strickland, Opt. Comm. 55, (1985), 447

Linear optics

(Solar radiation~ $0.1 W/cm^2$)

(Mourou, G.A., et al., *Exawatt-Zettawatt pulse generation and applications.* Optics Communications, 2012. **285**(5): p. 720-724)

Components of a CPA TeraWatt System

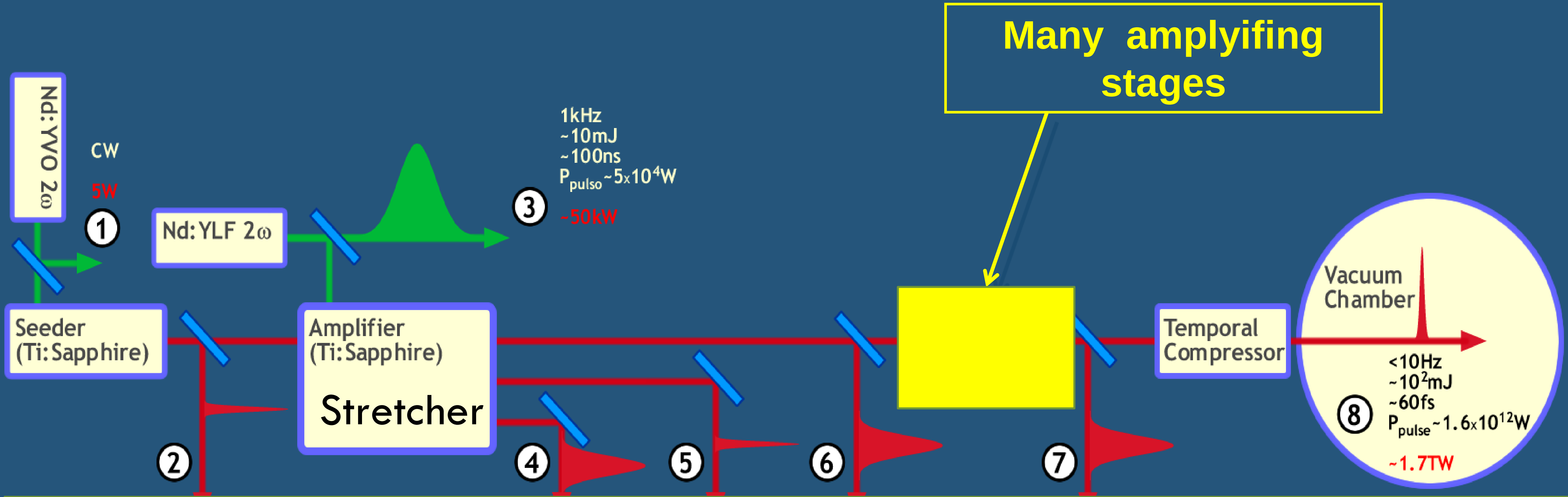

Components of IPEN CPA TeraWatt System

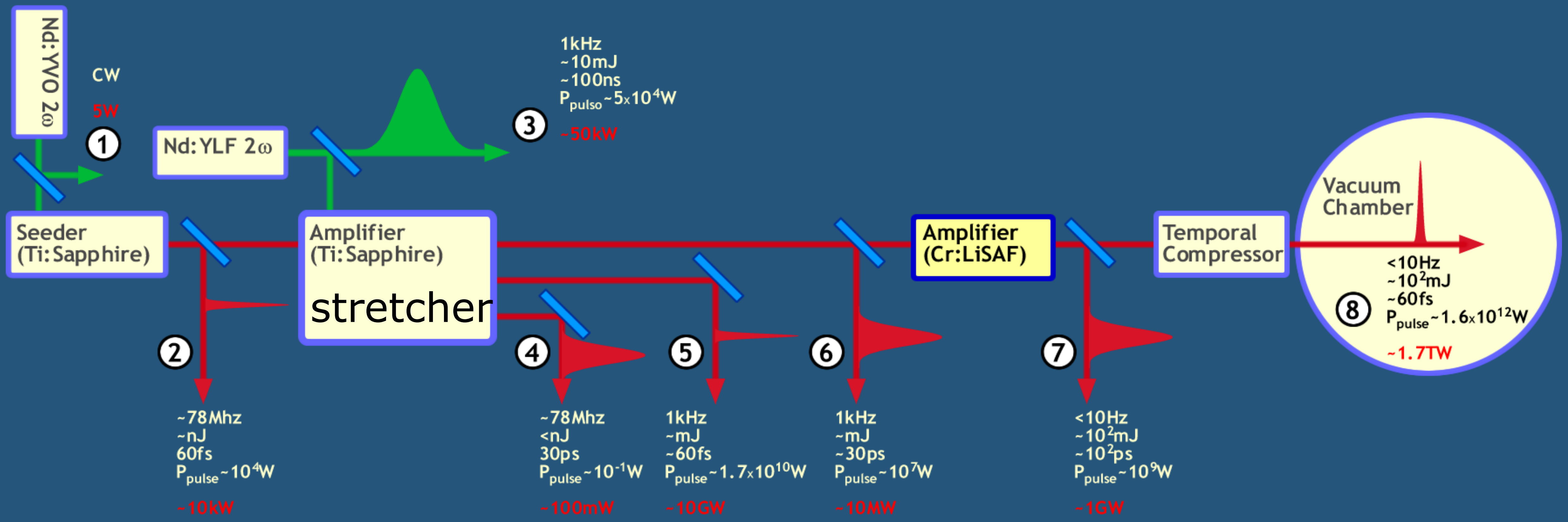

IPEN TABLE TOP TW = T^3

VISIT US at IPEN!

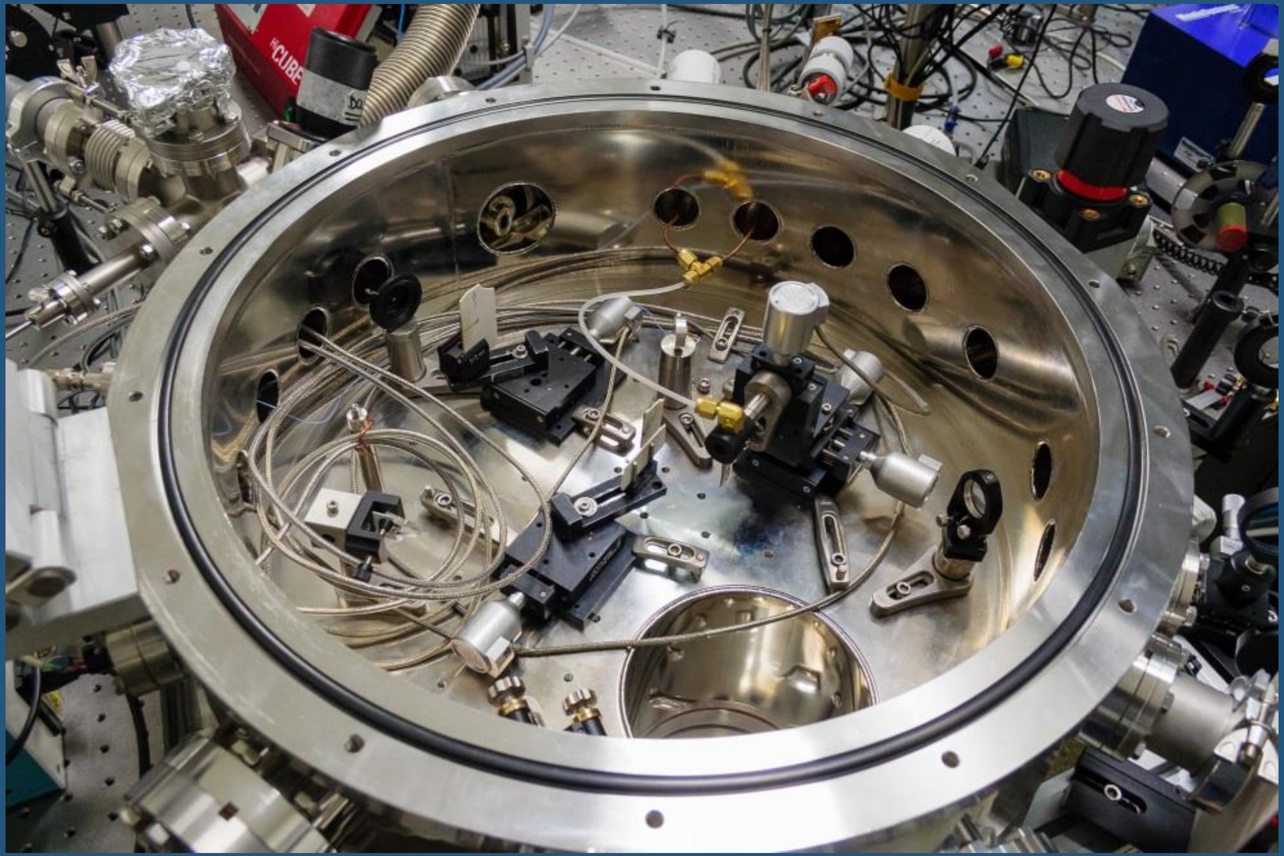

Vacuum chamber

amplifier

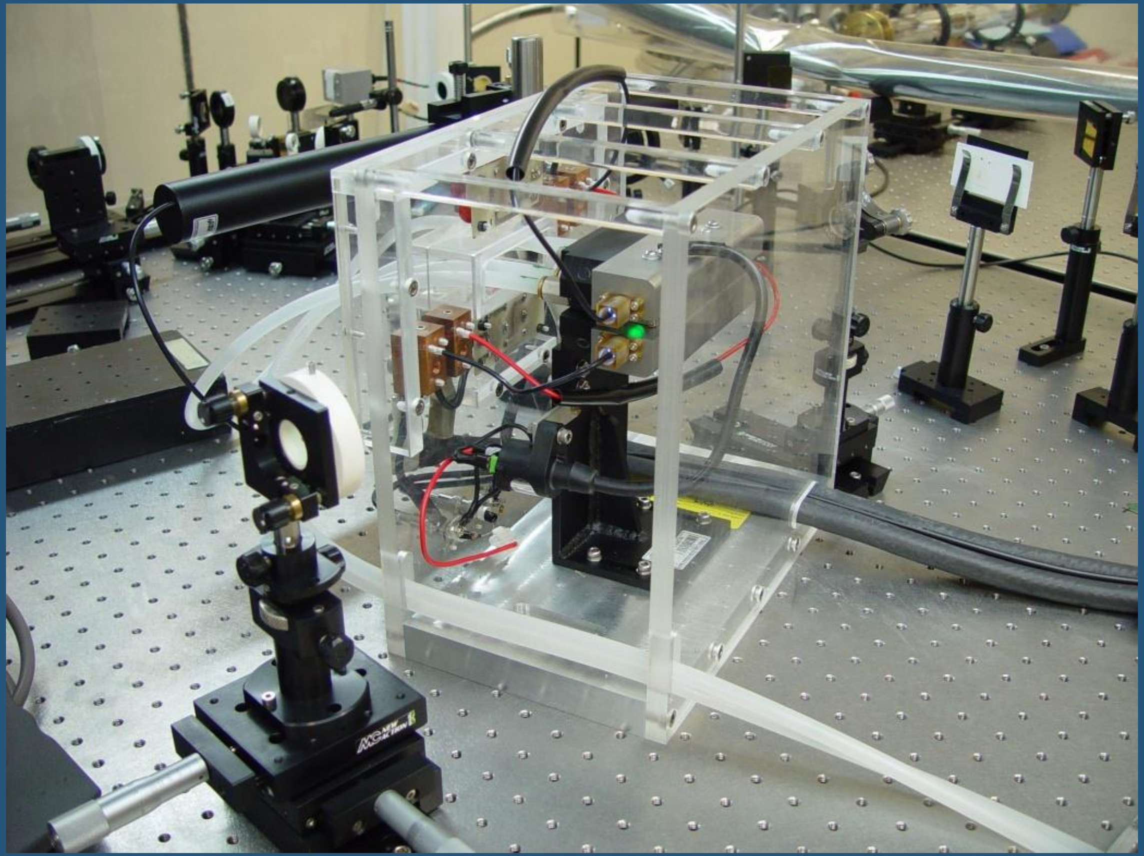

ACCELERATION IN THE OPTICAL LASER FIELD INTENSITY I AND TJHE ELECTRIC FIELD E

$$I = \Re e\left\{\frac{1}{2}E \times H^*\right\} = \frac{1}{2}c\epsilon_0|E|^2$$

For a plane wave the Electric peak amplitude is

$$E\,(\mathrm{V/cm}) = 27{,}5\,\sqrt{I\,(\mathrm{W/cm^2})}$$

Under the oscillation of the sinusoidal electic field,
The average kinetic energy U_P of the electron is:

$$\boldsymbol{U_P(MeV) = 9,3 \cdot 10^{-20} I(W/cm^2)\, \lambda(\mu m)^2}$$

LASER DIRECT IONIZATION - BOHR MODEL

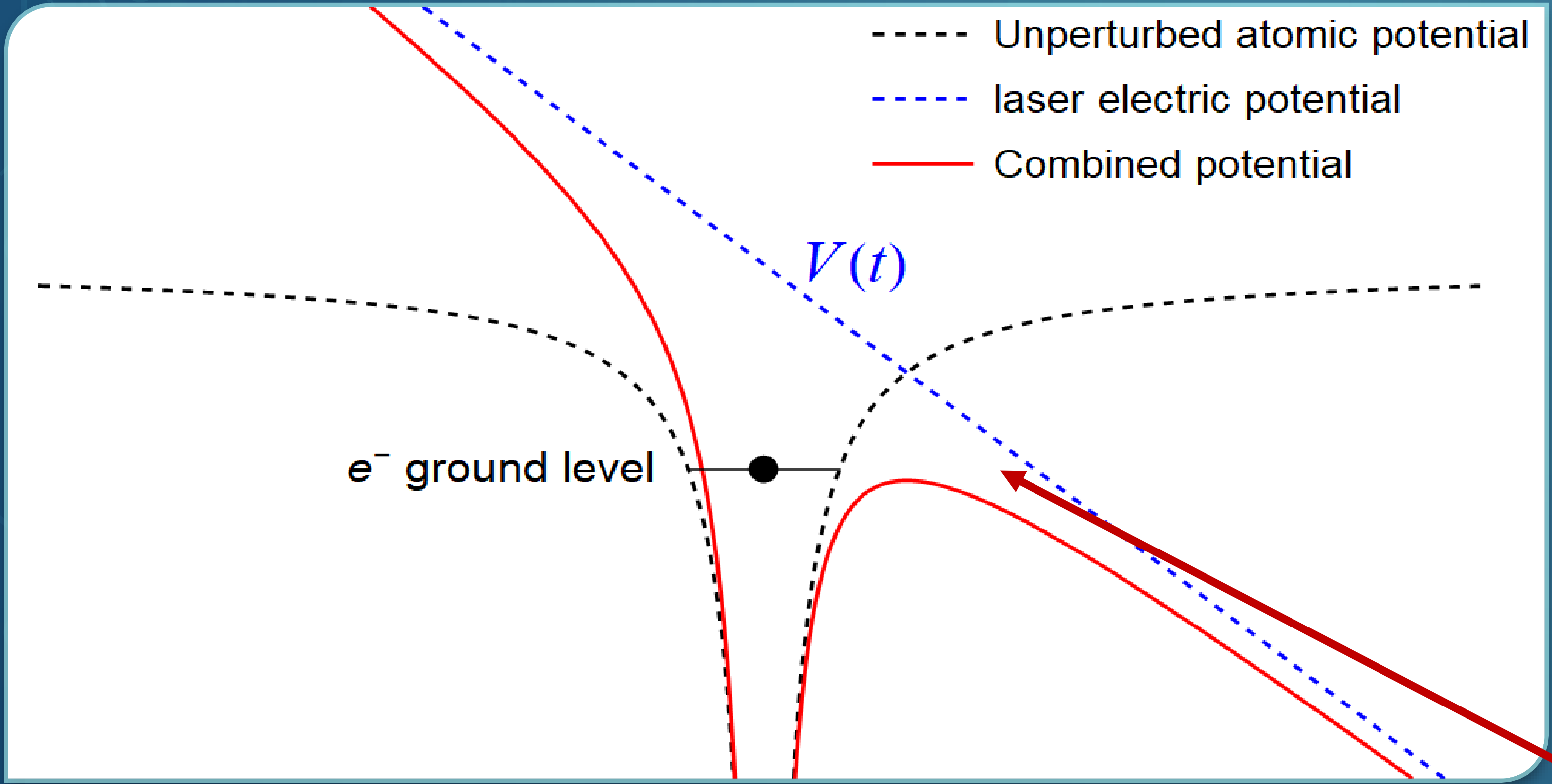

Binding energy is 13,6 eV

Atomic electrical field = 27.2 V / 0,5 Å

= 54,4 V/ Å = **5.44 GV/cm**

Supression of the electrostatic Coulomb barrier

Light Intensity for supression= $1.37 \cdot 10^{14}\ W/cm^2$

THRESHOLD FOR IONIZATION
I ~ 10^{14} W/CM^2

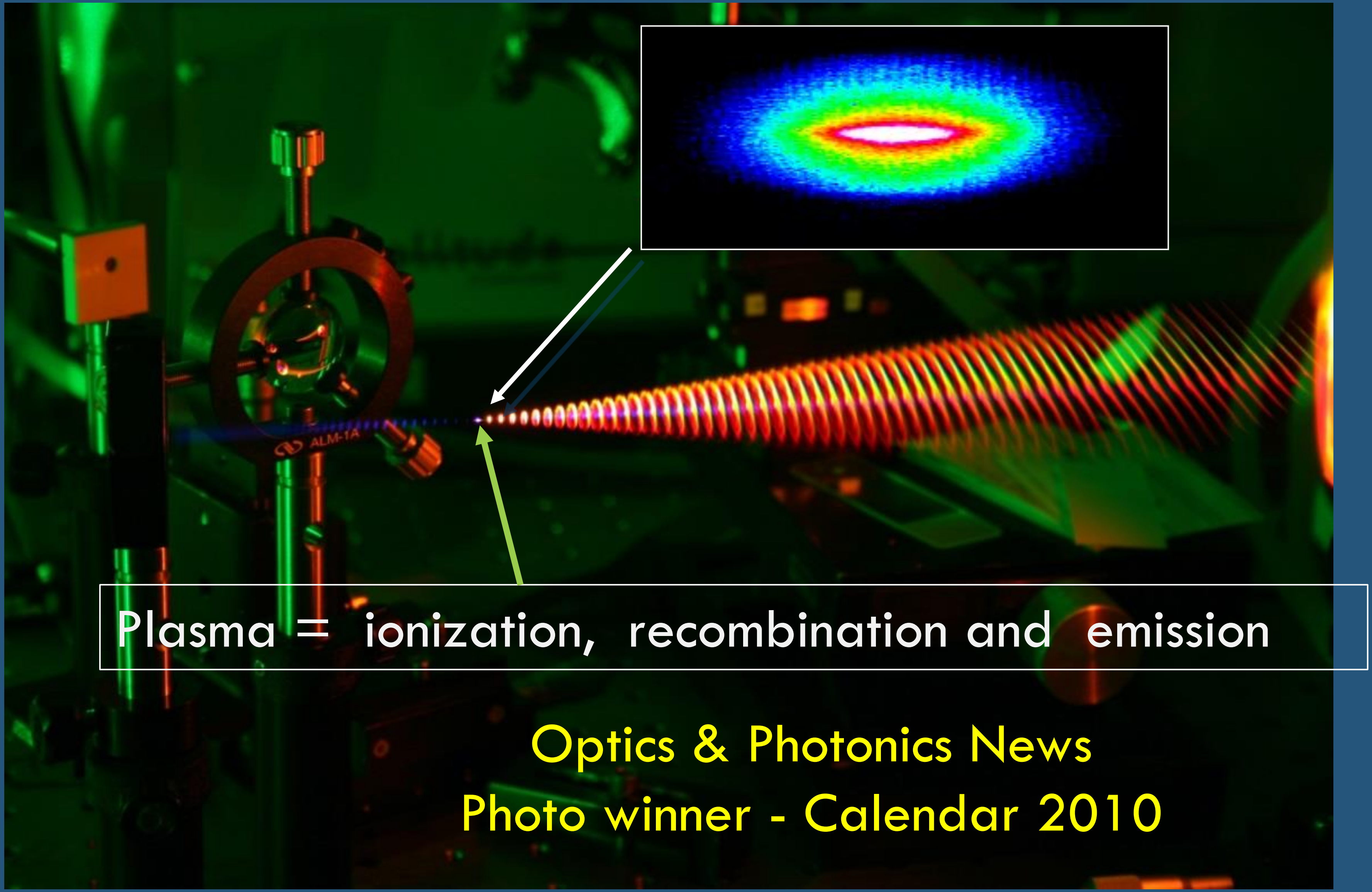

MAIN LASER ACCELERATION MECHANISMS

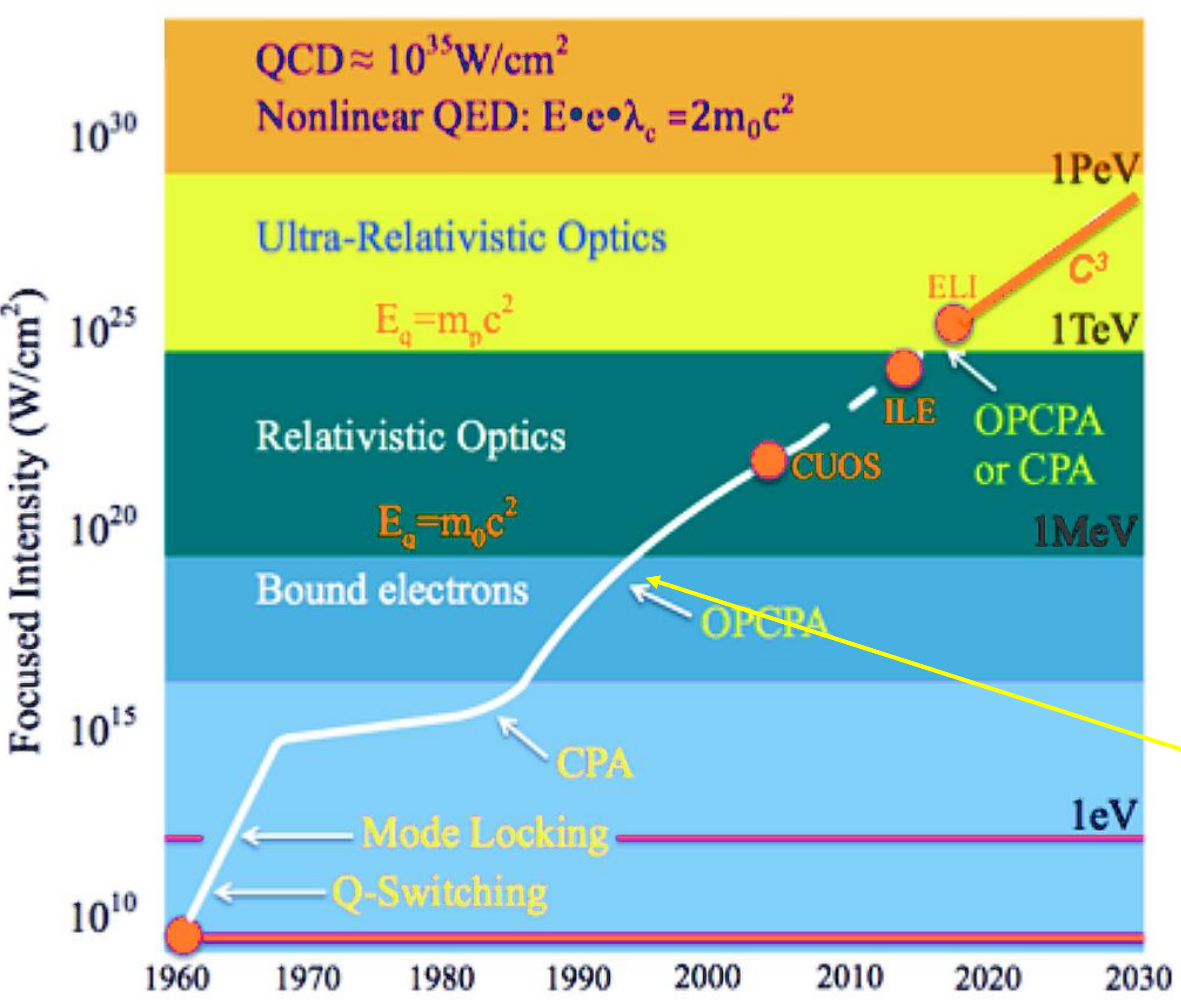

Ponderomotive Energy

due to the quivering motion

$$U_P(MeV) = 9,3 \cdot 10^{-20} I(W/cm^2)\, \lambda(\mu m)^2$$

At the Intensity of $\approx 9 \cdot 10^{18}$ W/cm^2 at 800 nm

The electron kinetic energy is equal to the rest mas 0,511 MeV

LASER DIRECT ACCELERATION - LORENTZ FORCE

$$\mathbf{F}_L = e(\mathbf{E} + \mathbf{v} \times \mathbf{B})$$

The second term (magnetic force)
is along the laser incident direction
Relativistic effect

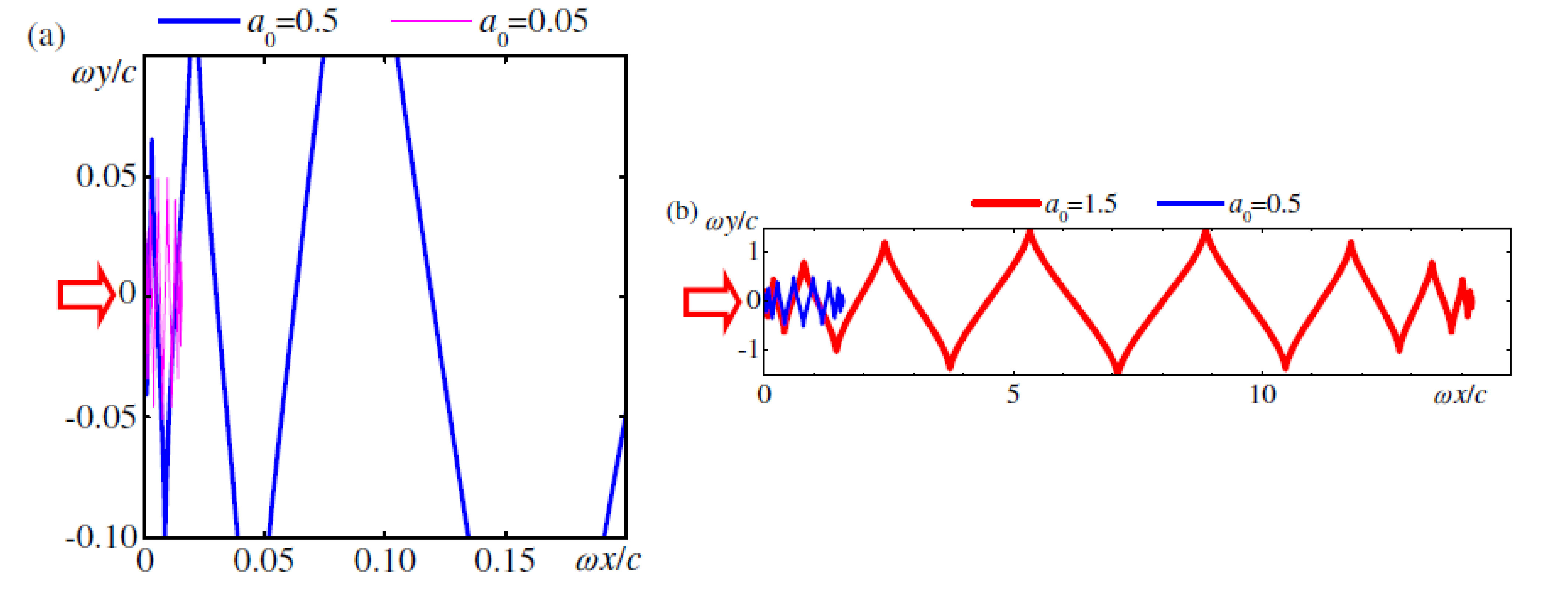

LASER WAKEFIELD ACCELERATION

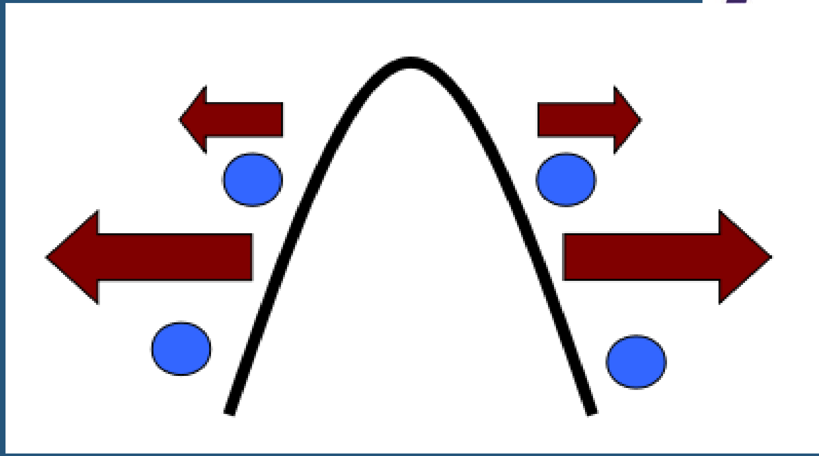

Laser with Gaussian Intensity Profile in a gas medium.

- Atoms/molecules are ionized ;
- The ionization front moves with the speed of the light and the ions remain in place;
- Electrons are forced out and then are pushed back to the axial position due to the attraction of the ions, eectrons oscillated around the equilibrium position with

$$\omega_p = \sqrt{\frac{n_e e^2}{m_e \epsilon_0}}$$ the plasma frequency and a wavelength $$\lambda_p = \frac{2\pi c}{\omega_p}$$

THE WAKEFIELD OF THE LASER-PLASMA INTERACTION

The frequency and the wavelenght of the wakefield depend only on the electron population, n_e

$$\omega_p = \sqrt{\frac{n_e e^2}{m_e \epsilon_0}}$$

$$\lambda_p = \frac{2\pi c}{\omega_p} = 3.4\ 10^{10}/\sqrt{n_e}$$

RESONANT OR BUBBLE REGIME

Laser wake field acceleration: the highly non-linear broken-wave regime, Appl. Phys. B 74, 355–361 (2002) a. pukhov meyer-ter-vehn

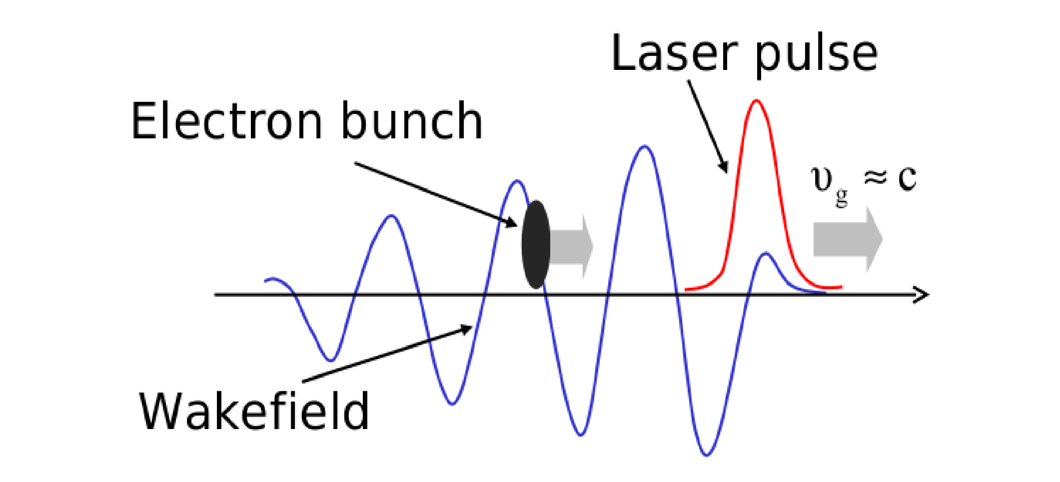

$\lambda/_2 = c.\Delta.t = w_0$ (the radius of the beam)

$I \geq 4.2\ 10^{18}$ W/cm^2 **=> P $\geq$ 120 TW**

for $w_0 = 10\ \mu$m

- C. G. R. Geddes, C. Toth, J. van Tilborg, E. Esarey, C. B. Schroeder, D. Bruhwiler, *et al.*, "High-quality electron beams from a laser wakefield accelerator using plasma-channel guiding," *Nature*, vol. 431, pp. 538-541, Sep 2004.
- S. P. D. Mangles, C. D. Murphy, Z. Najmudin, A. G. R. Thomas, J. L. Collier, A. E. Dangor, *et al.*, "Monoenergetic beams of relativistic electrons from intense laser-plasma interactions," *Nature*, vol. 431, pp. 535-538, Sep 2004.
- J. Faure, Y. Glinec, A. Pukhov, S. Kiselev, S. Gordienko, E. Lefebvre, *et al.*, "A laser-plasma accelerator producing monoenergetic electron beams," *Nature*, vol. 431, pp. 541-544, Sep 2004.

From the Nobel Prize Speech of Gerard Mourou

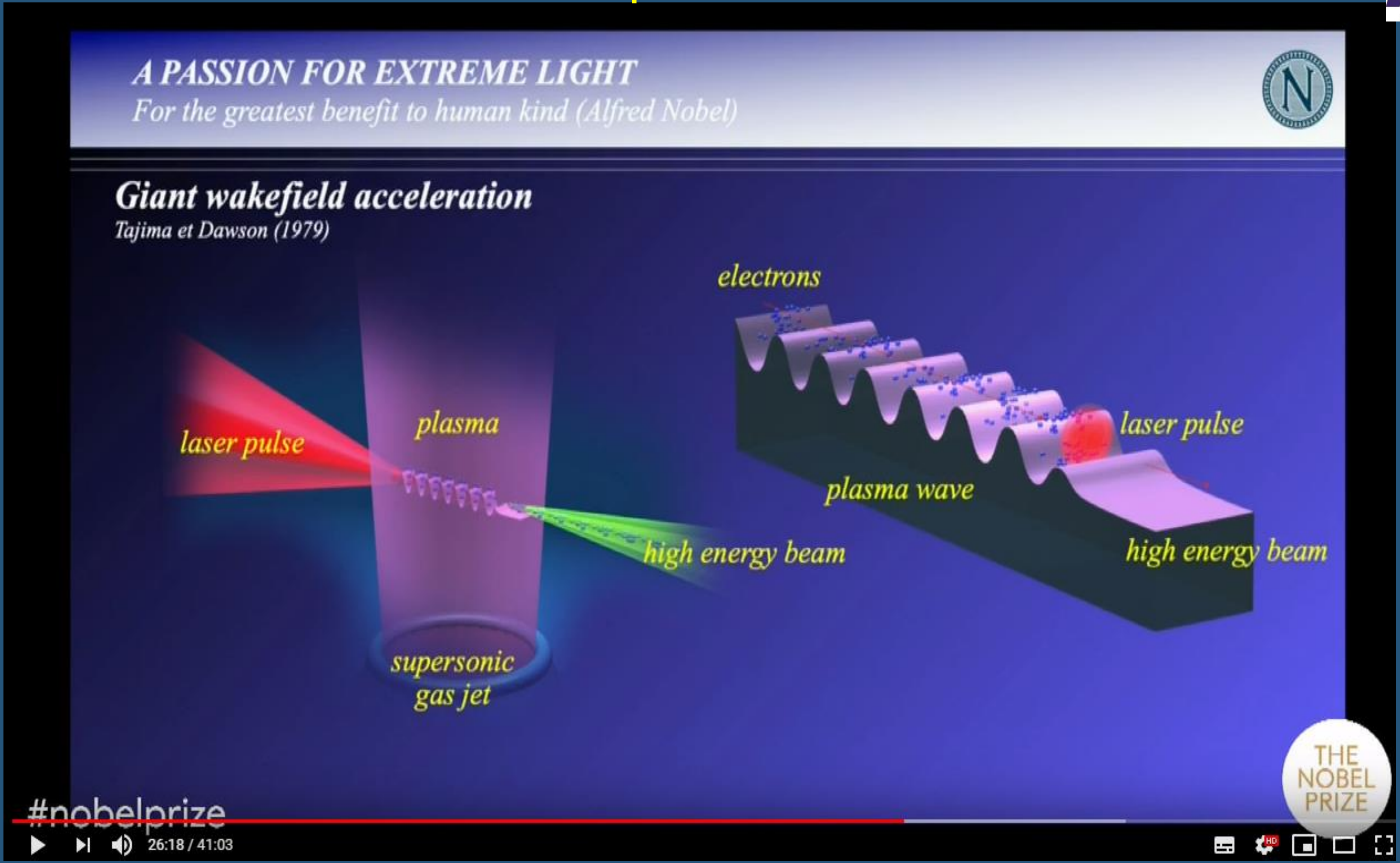

https://www.youtube.com/watch?v=W5Fz_BsWCjU

ENERGY OF THE ELECTRON IN THE LWPA

The maximum electrical field is

$$E_0(v/cm) = c.m_e.\omega_p/e \cong 0.96\sqrt{n_e(cm^{-3})}$$

For $n_e = 10^{18}$ cm^{-3} ➔ $E_0 = 96\,GV/cm$

(1 order of magnitude greater than the material limit)

The acceleration range is the dephasing length $T/2 = L/v_g - L/c$

With $T = 2.\pi/\omega_p$ and $v_g = c\left(1 - \frac{{\omega_p}^2}{\omega^2}\right)$

Therefore:

$$L_{max} = \frac{2c\pi\omega^2}{\omega_p^3}$$

The maximum kinetic energy is $E_m = e.E_0.L_m$

RESONANT OR BUBBLE REGIME

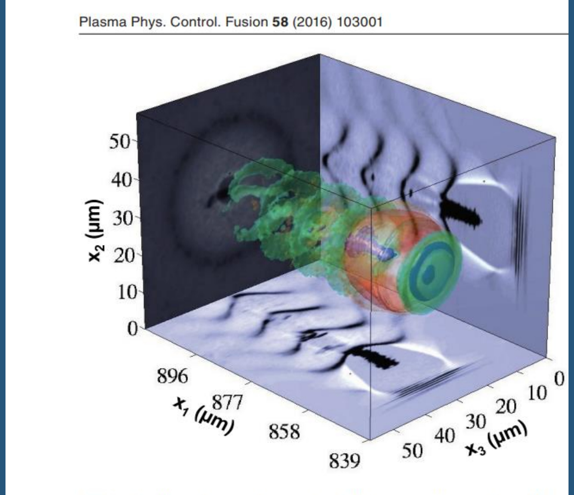

Figure 2. Illustration of laser wakefield acceleration in the bubble

- *fs duration*
- *low repetition rate*
- *Large Laser System*
- *Charge was 5 pC at 7.8 GeV and up to 62 pC in 6 GeV peaks, and typical beam divergence was 0.2 mrad.*
- *Gas pressure ~ 1/10 atmosphere*
- *Highly nonlinear regime for injection*

Raadt, et all and Leemans, W. P., "Petawatt laser guiding and electron beam acceleration to 8 GeV in a laser heated capillary discharge waveguide," Phys. Rev. Lett. 122, 084801 (Feb. 2019).

Few cm in LWPA compared to km long conventional accelerators!

INCREASING THE REPETITION AND DECREASING THE SIZE OF THE LASER SYSTEM

- Resonant Condition: $\lambda_p/2$ = c.Δ.t = w_0 = radius of the beam waist
- Scales with Δt^3 w_0 (area of the focus and length of acceleration)
- Therefore driving Optical power drops from PW to TW => kHz
- 24nA, few MeV , high pointing stability
- Jet nozzle size in the 100 μm range
- Limited by the plasma critical density@800nm ($1.7 10^{21}$ electrons/cm^3)

REQUIREMENTS FOR THE GAS JET NOZZLE

Laser beam in a gas plasma

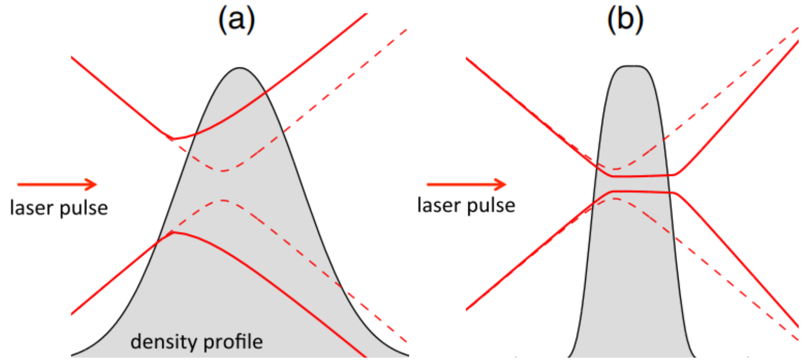

FIG. 1. Schematic of beam propagation issues in microscale jets. The dashed line represents the vacuum laser beam whereas the full line shows the beam size considering plasma effects. (a) The density gradients are large compared to z_R preventing the laser beam from reaching high intensity in the jet. (b) With sharper density gradients, coupling into the jet is optimized and the laser beam can reach higher intensities through self-focusing.

Laser beam in vacuum Rayleigth Parameter Z_R

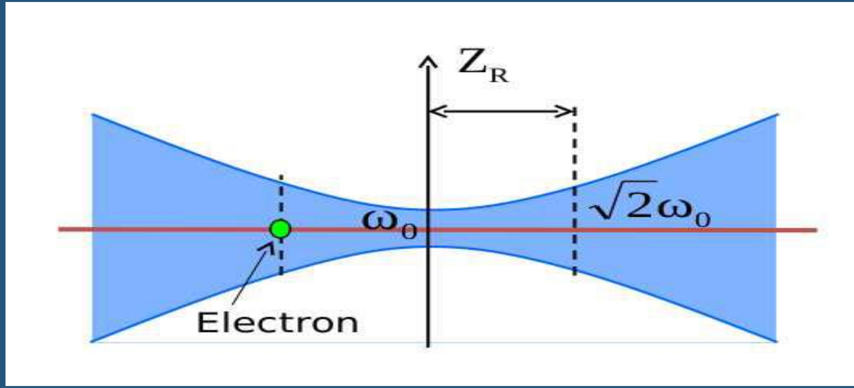

$$\eta = \sqrt{1 - \frac{n_e}{n_c}}$$

Gaussian profile and increasing intensities **defocusing**

High-charge relativistic electron bunches from a kHz laser-plasma accelerator, D. Gustas et al,
PHYSICAL REVIEW ACCELERATORS AND BEAMS 21, 013401 (2018)

RECENT DEVELOPMENTS

All need de Laval jet nozzles!

Electron Acceleration with sub TW Laser with high density gas jets

- F. Salehi et all "MeV electron acceleration at 1 kHz with <10 mJ laser pulses," *Opt. Lett.* **42**, pp.215-218 (2017)
- Goers, A.J., et al., Multi-MeV Electron Acceleration by Subterawatt Laser Pulses. Phys Rev Lett, 2015. 115(19): p. 194802.
- , J Faure et all, Plasma Phys, A review of recent progress on laser-plasma acceleration at kHz repetition rate. . Control. Fusion 61 (2019) 014012
- D. Gustas. High-charge relativistic electron bunches from a kHz laser-plasma accelerator, PHYSICAL REVIEW ACCELERATORS AND BEAMS 21, 013401 (2018)

Proton Acceleration witn high density liquids and gases

- P. Puyuelo Valdé et all , "Laser driven ion acceleration in high-density gas jets", Proc. SPIE 11037, 10 (2019).
- John T Morrison1 et all MeV proton acceleration at kHz repetition rate from ultra-intense laser liquid interaction. New J. Phys. 20 (2018) 022001

REQUIRENTS FOR THE JET NOZZLE

Short pulse => high plasma frequency => high n_e

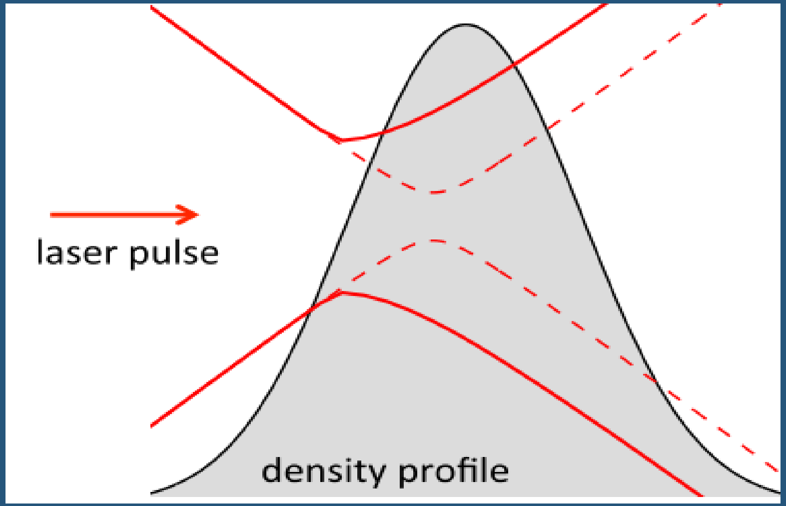

- Short homogeneous acceleration path (≈100 μm plasma path)
- Ramp Shorter than the Z_R ((≈10 μm thick) – interface

  between the jet nozzle and the vacuum

  Focused intensities above the relativistic self focusing

$$P_c \simeq 17{,}4\left(\frac{\omega}{\omega_p}\right)^2 GW$$

$$= 17{,}4\left(\frac{n_c}{n_e}\right)\mathrm{GW}$$

$$\eta = \sqrt{1 - \frac{\omega_p^2}{\gamma\omega^2}}$$

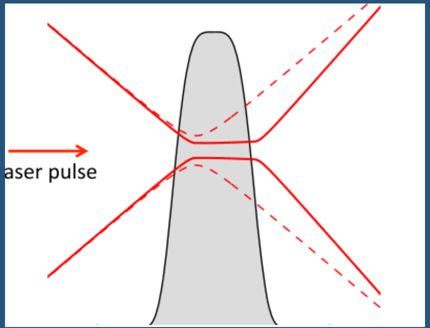

QUASI-1D MODEL FOR DE LAVAL JET NOZZLE ISENTROPIC FLOW

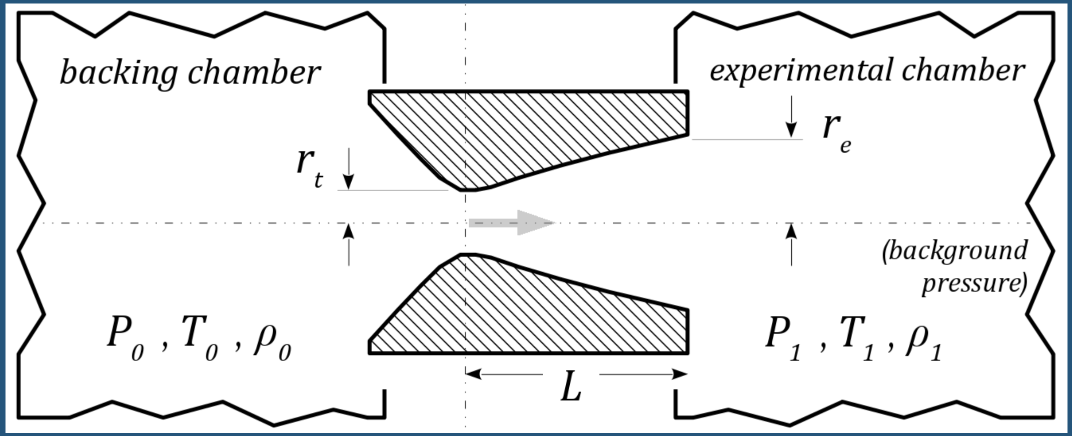

Sylla, Fet all V. "Development and characterization of very dense submillimetric gas jets for laser-plasma interaction," Rev. Sci. Instrum., 83, pp. 033507, 2012.

The important parameter is the Mach NUMBER M *and the backing pressure*

$$\frac{A_e}{A_t} = \frac{1}{M}\left[\frac{2+(\gamma-1)M^2}{\gamma+1}\right]^{\frac{\gamma+1}{2(\gamma-1)}}$$

$$\dot{m} = A_t P_0 \sqrt{\frac{\gamma}{R T_0}}\left(\frac{2}{\gamma+1}\right)^{\frac{\gamma+1}{2(\gamma-1)}}$$

$$\frac{\rho}{\rho_0} = \frac{1}{M}\left[\frac{\gamma+1}{2+(\gamma-1)M^2}\right]^{\frac{1}{(\gamma-1)}}$$

HOME MADE DE LAVAL JET NOZZLE

- homemade ultrafast laser machining

system to etch a conic-shaped hole with a high aspect ratio

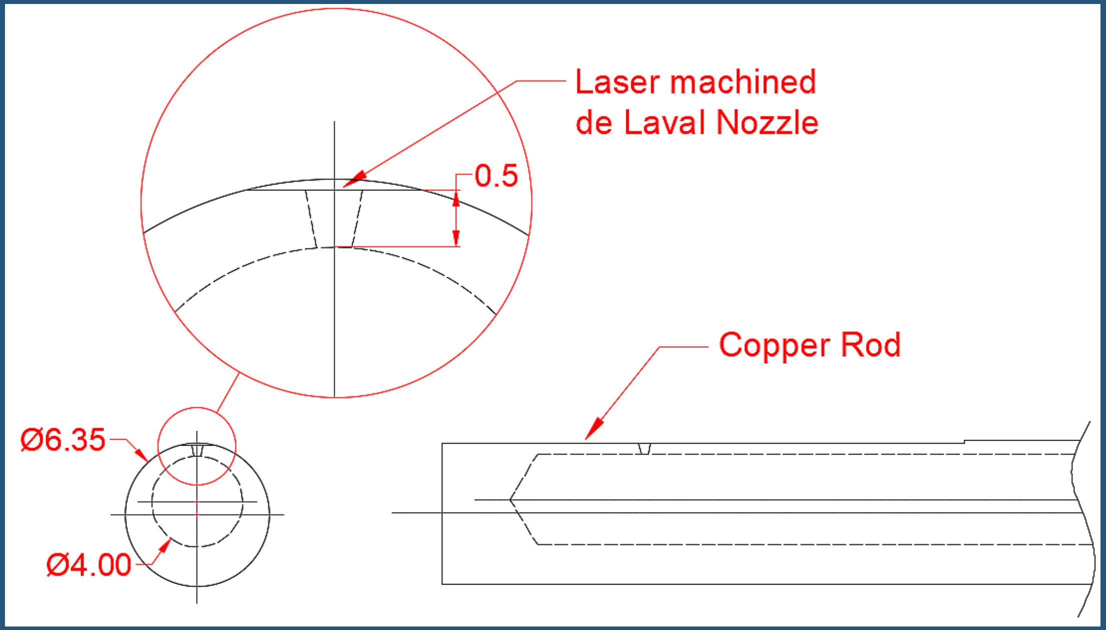

Assuming a N_2 backing pressure of 15 bar and using (1) to (4), we expected to obtain the mass ($\dot{m}$) and flow (v_1) rates, number density (n) and angle (α) shown in Table I.

TABLE I. CALCULATED CHARACTERISTICS FOR THE MANUFACTURED NOZZLE, MACH 2.5.

$\dot{m}$ (kg/s)	v_1 (m^3/h)	n (cm^{-3})	n_0/n	α (deg)
6×10^{-5}	19.0	6×10^{19}	12	23.6

The nozzle exit diameter is approximately 250 µm *M*= 2.5

Laser Processing Center-fs pulses and nm precision

Texturization

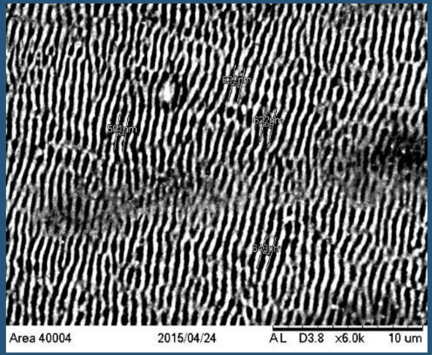

Titanium

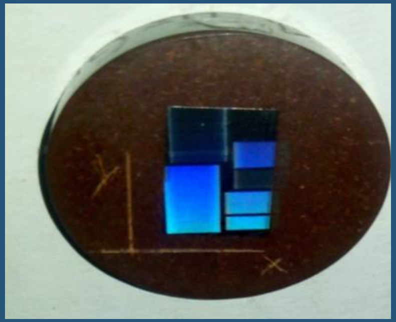

Microchannel etched in glass

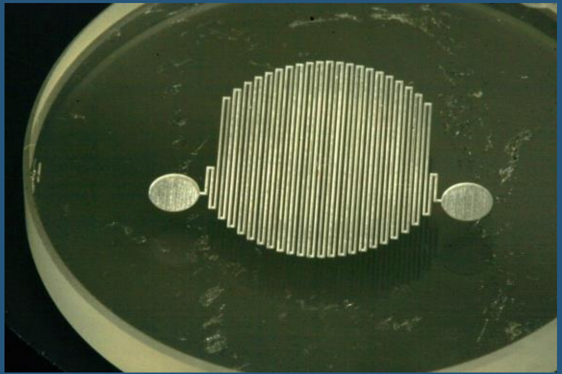

Grant FAPESP 13/26113-6
Dr. Wagner de Rossi

10 kHz, 30 fs, P = 2 W, Peak Power = 10 GW, 20 fs

GAS JET CHARACTERIZATION

Schlieren imaging
&
Mach–Zehnder interferometry

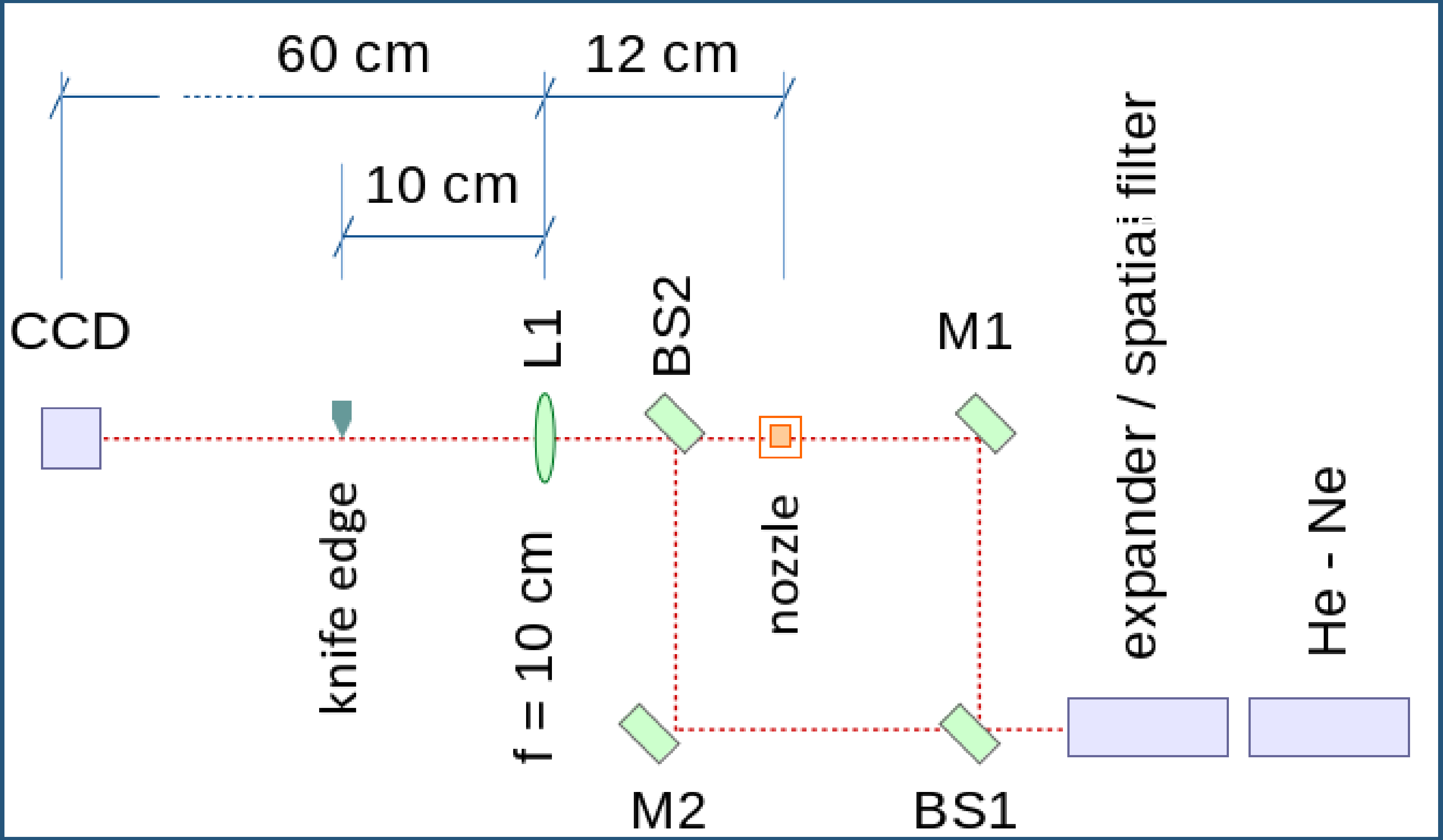

- *Schlieren* imaging

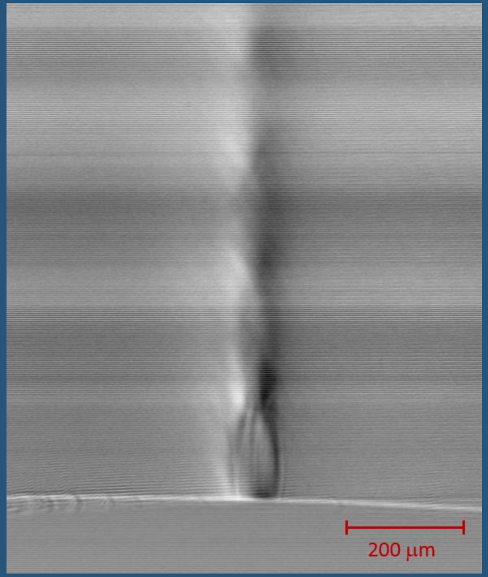

Mach–Zehnder interferometry

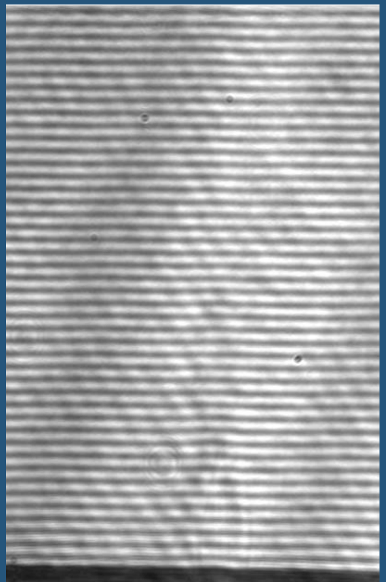

The prssure in the gas jet

At 1 Atm, gas density $2.5\ 10^{19}$ species/cm^3

For N_2 :
$5\ 10^{19}$ atoms/cm^3@1 Bar

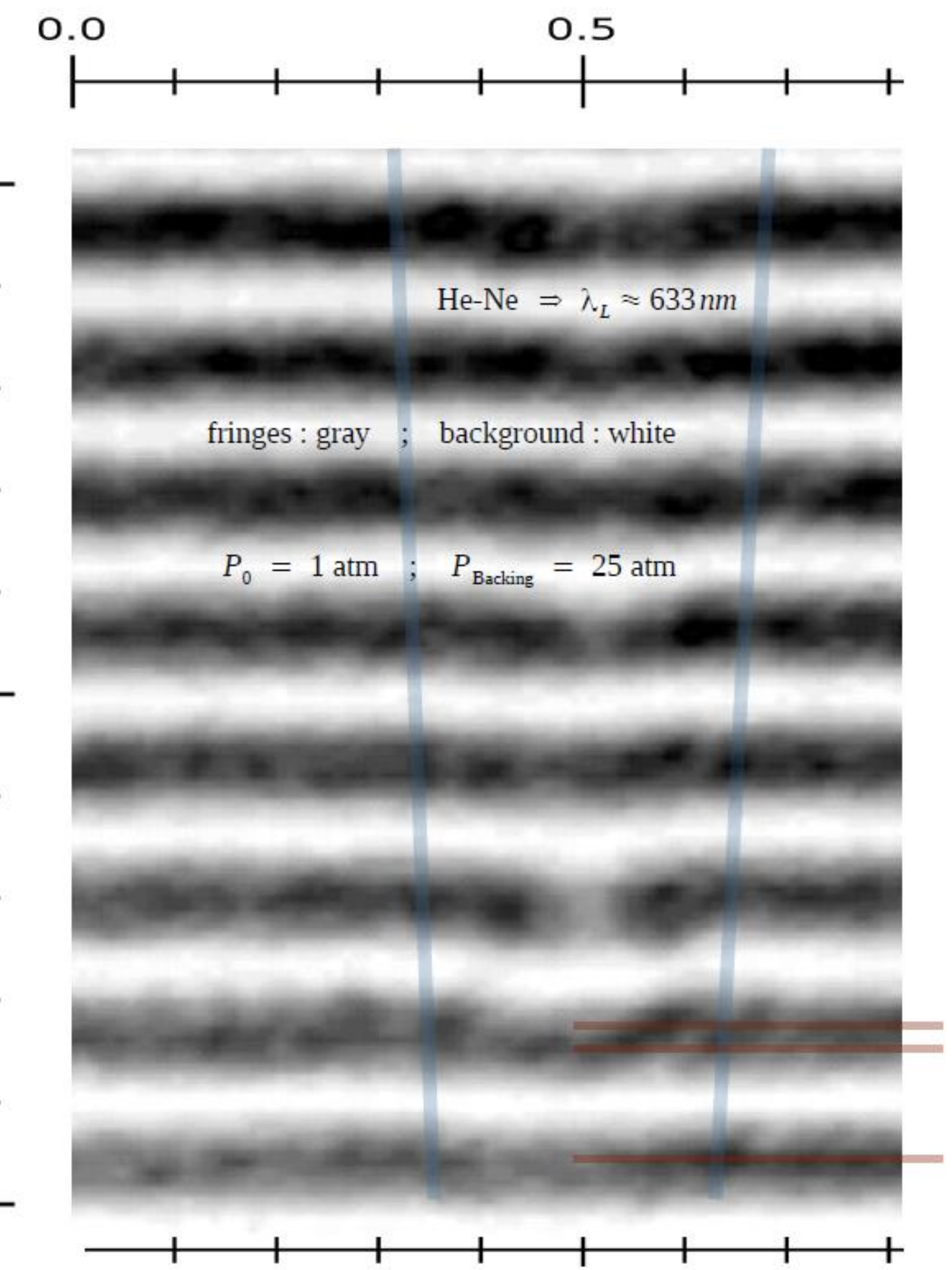

from figure (red lines):

$$\Delta\Phi = 2\pi \frac{\Delta OPL}{\lambda_L} \approx \frac{2\pi}{5}$$

therefore:

$$\Delta OPL \approx \Delta n \Delta s \approx 127\ nm$$

from figure (blue lines):

$$\Delta s \approx 275\mu m \quad \Rightarrow \quad \Delta n \approx 5e\text{-}4$$

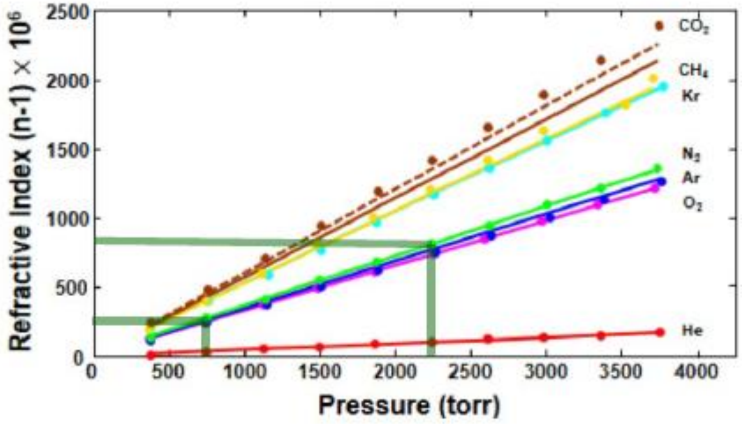

thus: $\Delta P \approx$ 1500 torr $\approx$ 2 atm

REFERENCES:

- *Sang, B H et al. "Pressure-Dependent Refractive Indices of Gases by THz Time-Domain Spectroscopy." Optics Express 24 (25):29040.*
- *Couperus, J P et al. "Tomographic Characterisation of Gas-Jet Targets for Laser Wakefield Acceleration." Nuclear Instruments and Methods in Physics Research, Section A 830, 504–9, 2016*

2017-01-18 Puig

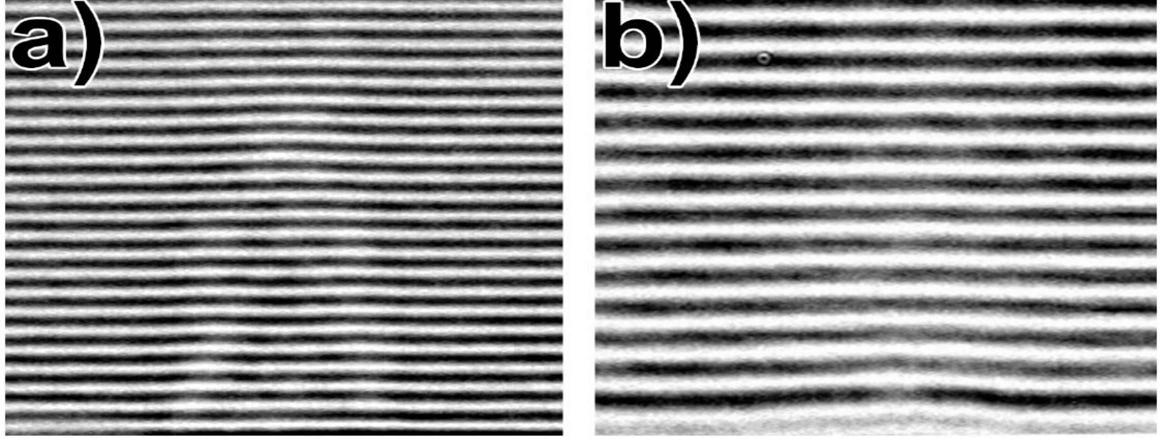

Fig. 5. Typical Mach-Zehnder interferograms for 633 nm HeNe continuous beam transmission through the cross section of the gas jet near the exit of our Mach 2.5 nozzle, in background pressures of a) 1 atm and b) 10 mbar. The nozzle exit is in the lower edge of the frame and both images cover the first 500 µm of the jet; the applied backing gas pressure was 15 bars.

Laser Pulse

Superposition of the Schlieren and plasma images, showing where typically the plasma forms.

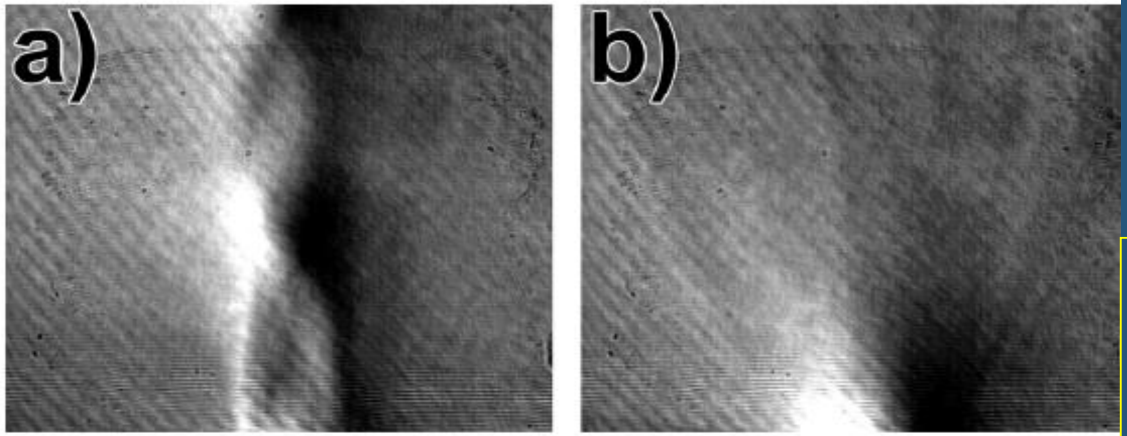

Fig. 4. Typical Schlieren image of the gas flow near the exit of ou Mach 2.5 nozzle, in background pressures of a) 1 atm and b) 10 mbar. The nozzle exit is in the lower edge of the frame, and both images cover th first 750 µm of the jet; the applied backing pressure was 15 bars.

- M = 2.2 instead of the predicted 2.5;
- ionization states up to N^{3+}.
- atomic density of ~1×10^{20} cm^{-3}
- Max. electron density~ 6×10^{20} cm^{-3}

Laser Induced Breakdown Spectroscopy - LIBS

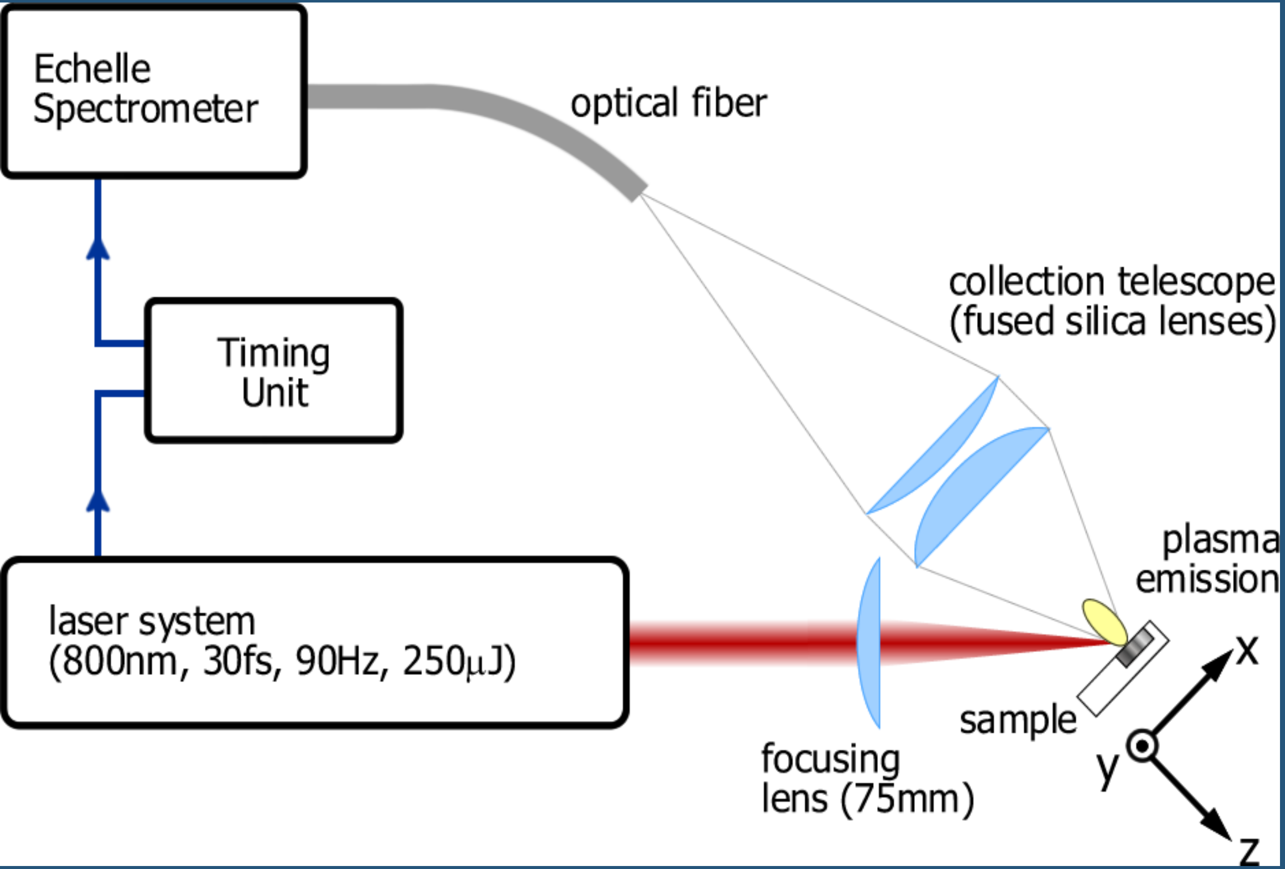

Grant FAPESP 04/15965-2

Evaluation of laser induced breakdown spectroscopy for the determination of macronutrients in plant materials, Spectrochimica Acta Part b, 63 (2008)1151- 1158

Nitrogen Spectra

Presence of single, double and triple Ionization states.

Ay 50 ns (10^6 pulse durations neutral N)

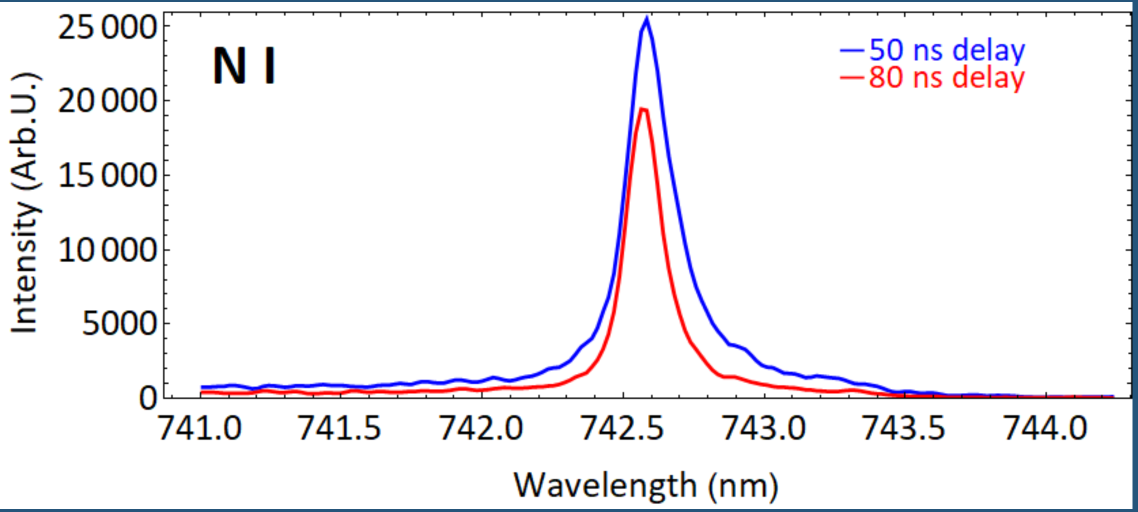

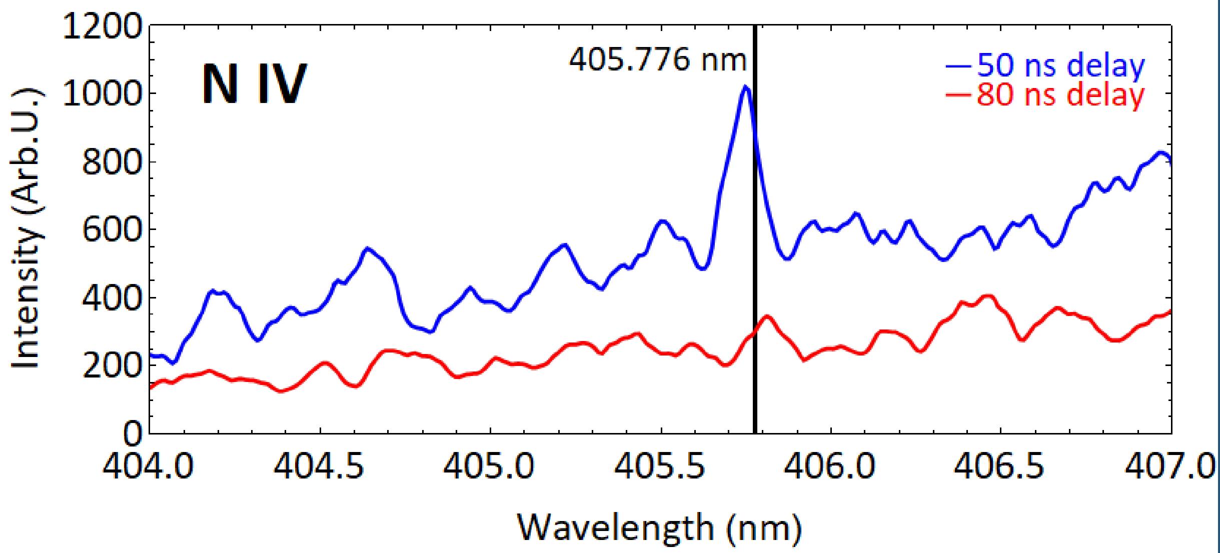

JET NOZZLES MADE BY FS LASER MACHINING WITH DUAL FIT – IPEN AND UNL

ipen

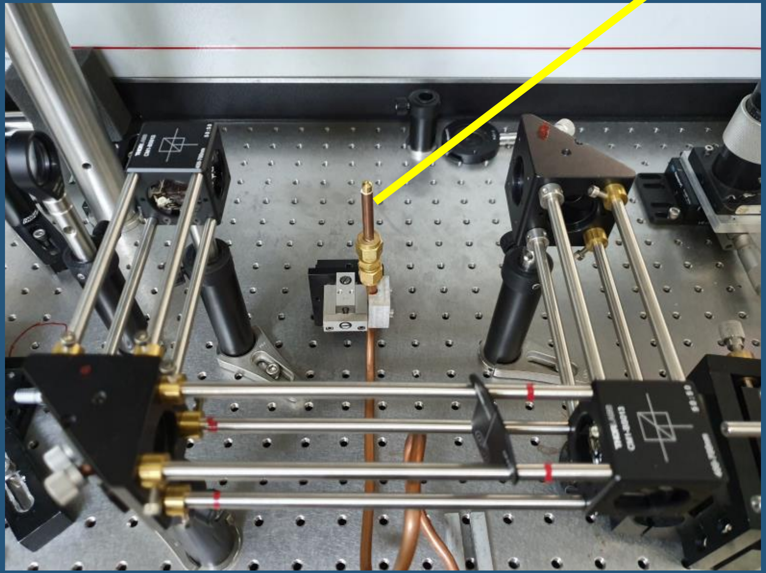

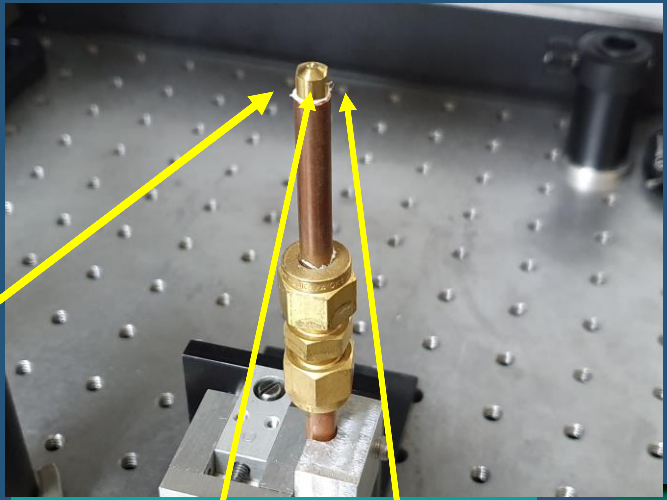

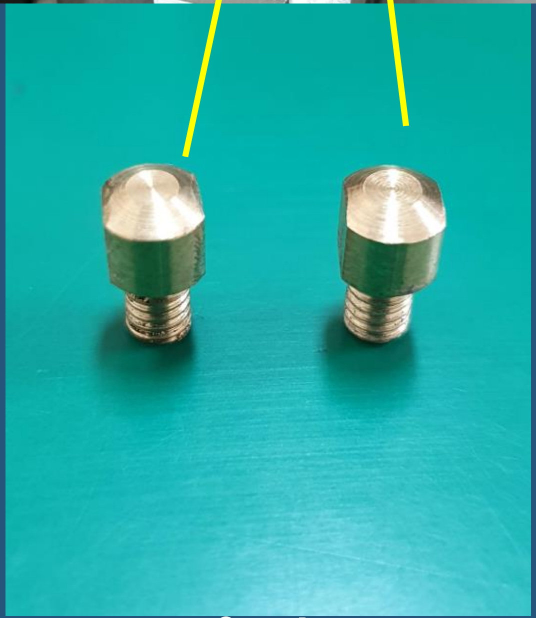

UNL flange

On going experiment – generation of electrons with our conditions

SELF MODULATED REGIME

BUBBLE REGIME NEEDS HIGH POWER

- Non-resonant condition $\lambda_{\mathrm{p}}/2 < c \times \Delta t$
- Short acceleration path (≈100 μm plasma path)
- Ramp Shorter than the ZR ((≈10 μm thick) – interface between the jet nozzle and the vacuum (de Laval nozzle)
- High repetition rates and high gas flows (no need for gas pulses)

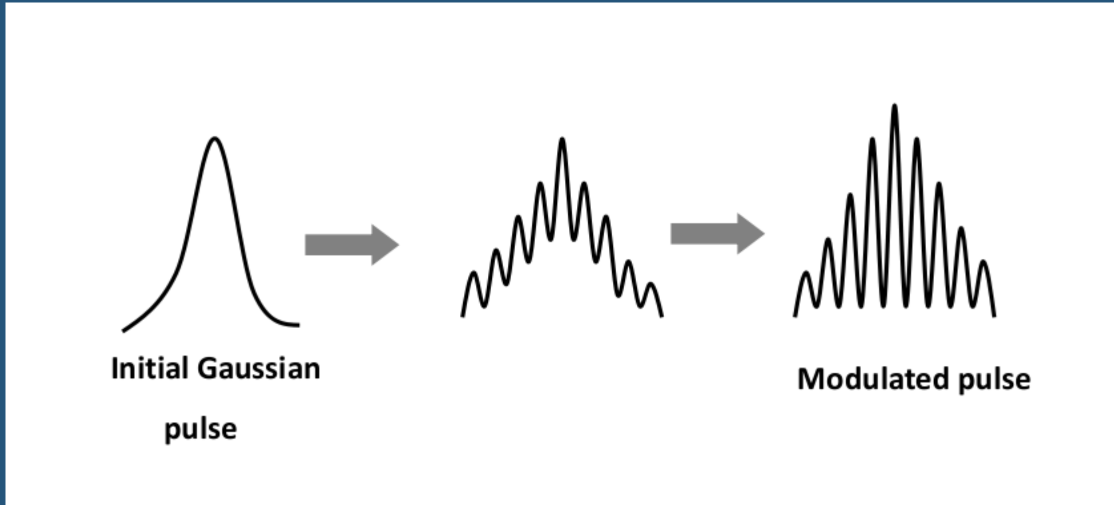

Self-modulated laser wakefield mechanism. The initial laser pulse undergoes density modulation instability and breaks up into a train of shorter pulse with width λ_p.

SELF MODULATED REGIME

Electron injection needs laser power higher than the critical power P_c

$$P_c \simeq 17{,}4\left(\frac{\omega}{\omega_p}\right)^2 GW = 17{,}4\left(\frac{n_c}{n_e}\right)\mathrm{GW}$$

=> high plasma frequency=>high electron density!

PIC SIMULATIONS (FBPIC) – E. PUIG (ITA)

Simulations using code FBPIC [R1, R2] – **"SM-LWFA FBPIC 4TW HE 5E19"**

Edison Puig Maldonado – Instituto Tecnológico de Aeronáutica – ITA, in collaboration with IPEN/CNEN-SP.

Wavelength λ [μm] = 0.80
Critical density, n_c [cm⁻³] = 1.75E+21
Laser beam M² = 1.00
n_i = number of ionizations ≤ 2

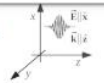

	PARAMETER	VALUE	CELLS WITH DARK BACKGROUND → PIC INPUT PARAMETERS
PHYSICAL	ε [mJ]	200	Pulse energy
	Δt [fs]	50	Pulse duration
	w_0 [μm]	5	Incident beamwaist (in vacuum)
	z_1 [μm]	10	Start position of the ramp 1 of gas densities
	$z_2 - z_1$ [μm]	20	Length of the ramp 1 of gas densities
	z_3 [μm]	200	Start position of the ramp 2 of gas densities
	$z_4 - z_3$ [μm]	20	Length of the ramp 2 of gas densities
	z_{FOC} [μm]	100	Position of laser focus if vacuum
	z_0 [μm]	10	Start position for the laser pulse
	n_{ATOMS} [cm⁻³]	2.5E+19	Nominal maximum density of atoms
CALCULATED	v_G / c	0.99	Plasma group velocity: $v_G = c\cdot(1 - n / n_c)^{1/2}$, $n = n_i \cdot n_{atoms}$
	b [μm]	196	Confocal parameter: $2\pi w_0^2 / M^2 \lambda$
	P_L [TW]	4.0	Peak power: $\varepsilon/\Delta t$
	A [cm²]	8E-07	Beamwaist area: $\pi \cdot w_0^2$
	I_L [W cm⁻²]	5E+18	Laser intensity: P_L/A
	L_{RMS} [μm]	15	Pulse length: $L_{RMS} \approx c\cdot\Delta t$
	λ_P [μm]	5	Plasma wavelength: $\lambda_P \approx 2\pi c/\omega_P = (2\pi c/e)\cdot(\epsilon_0 m_e/n)^{1/2}$
	a_0	1.6	Laser amplitude: $a_0 \approx 8.6\times10^{-10}(I_L\cdot(\lambda[\mu m])^2)^{1/2}$
	L_D [μm]	82	Dephasing length: $L_D \approx \lambda_P^3 / 2\lambda^2$
	P_C [TW]	0.6	Critical power for self-focusing: P_C [GW] = 17 (n_c/n) = 17 $(\omega/\omega_P)^2$
	w_{SF} [μm]	1.0	Estimated self-focused beamwaist
	A_{SF} [cm²]	3E-08	Estimated self-focused area
	I_{SF} [W cm⁻²]	1E+20	Estimated self-focused intensity
	a_{SF}	7.8	Estimated self-focused laser amplitude
	a_{WB}	5.2	Estimated laser amplitude for wave breaking: $a_0 \approx (2\,\omega/\omega_p)^{2/3}$
	ΔW [MeV]	43	Estimated maximum energy gain ΔW [MeV] $\approx 38\cdot(P_L/P_C)^{-2/3}\cdot P_L$ [TW] (OBS. 1)
NUMERICAL COMPUTING ★	$Z_{MAX} - Z_{MIN}$ [μm]	50	Length of the simulation box
	R_{MAX} [μm]	20	Simulation box radius
	N_Z (× 1000)	1.3	Number of grid points along Z
	N_R (× 1000)	0.4	Number of grid points along R
	N_M	3	Number of azimuthal modes
	V_{WINDOW} (c)	0.97	Speed of the moving window
	$L_{INTERACT}$ [μm]	300	Simulation length
	T_S [as]	133	The simulation timestep
	D_{PERIOD}	200	Interval for diagnostics [timesteps]
RESULTS	Size [GB]	10.4	Simulation data size
	Total time	09:09:33	Simulation run time (Debian 10, I-7 7700, 4-cpu, 3.6 GHz 16 GB – no GPU)
	LWF [μm]	80 to 140	Z-position for the onset of LWF (note: ion cavity, then wakefield)
	$\tilde{u}_Z$ [$m_e\cdot c$]	6	Median of Z-momentum distribution, from the graphs of u_Z
	u_Z^{MAX} [$m_e\cdot c$]	80	Maximum of Z-momentum distribution, from the graphs of u_Z
	K [MeV]	3	Reference kinetic energy, $K = 0.51\cdot((\tilde{u}_Z^2 + 1)^{1/2} - 1)$
	K^{MAX} [MeV]	40	Maximum kinetic energy, $K^{MÁX} = 0.51\cdot((\tilde{u}_Z^{MÁX} + 1)^{1/2} - 1)$
	Q [pC]	800	Bunch charge

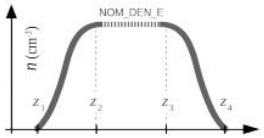

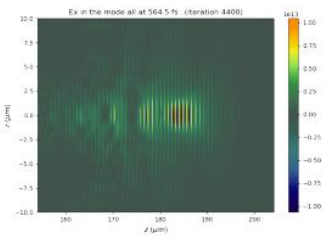

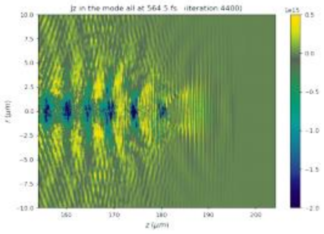

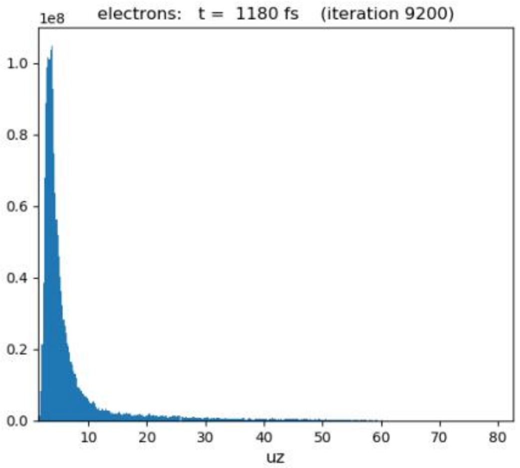

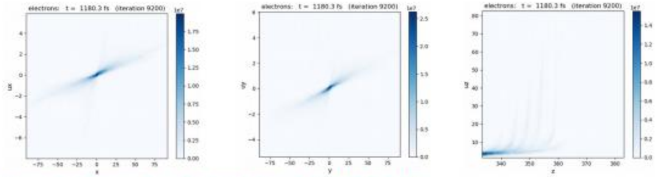

★ numerical computing parameters loosely following UCLA criteria: 20 pts/λ and 20 pts/w₀ (≈ 1 μm due to self focusing). See: Shaw et al. Plasma Phys. Control. Fusion 58 034008 (2016)

(OBS. 1) Lu et al. Physical Review Special Topics - Accelerators and Beams 10, 1–12 (2007) – http://doi.org/10.1103/PhysRevSTAB.10.061301

SM-LWFA_FBPIC_4TW_HE_5E19 19/09/2019 09:25:01 1 / 1

Output along the propagation and traversal axis:

- Net Electricl field
- Net Charges
- Net current
- Net Momentum of the electrons

PIC SIMULATIONS (FBPIC) – **E. PUIG (ITA)**
SIMULATION PARAMETERS

Laser
200 mJ, 50 fs, 4 TW
Wavelength 0.8 μm
Spot radius: 5 μm, Z_R = 80 μm,
$2Z_R$ = 160 μm,
Area~8 10^{-7} cm^2, I ~ 5 , 10^{18} W/cm^2
Laser pulse length= 15 μm;

Gas Jet
He, 1 atm
2,5 10^{19} atoms/cm^3
5 10^{19} electrons/cm^3
Ramp: 20 μm
Path: 180 μm

Interaction parameters:
V_g = 0.99. c
Plasma wavelength 5 μm
Dephasing length: 82 μm
Critical power for self focusing: 0.6 TW
Self fosusing intensity: 1. 10^{20} W/cm^2 >> 9. 10^{18}

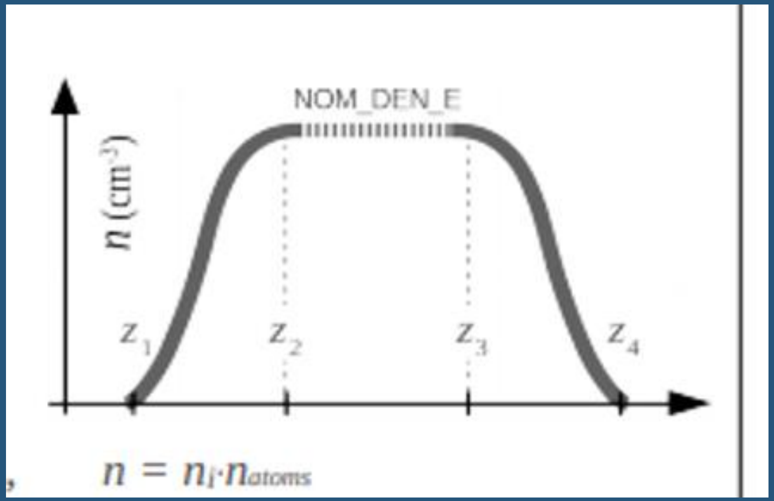

The porfile of the gaussian beam is visible

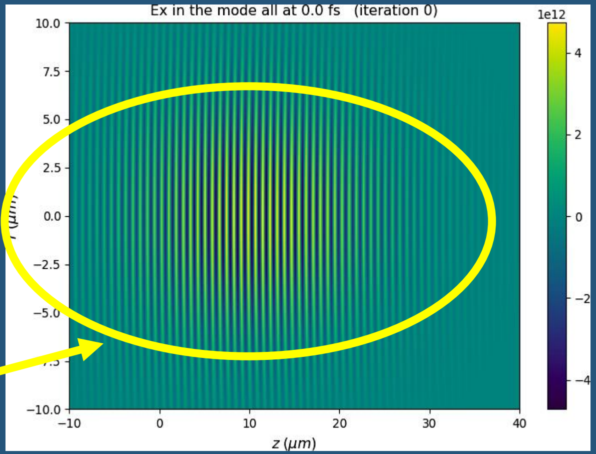

Electric Field (V/m)

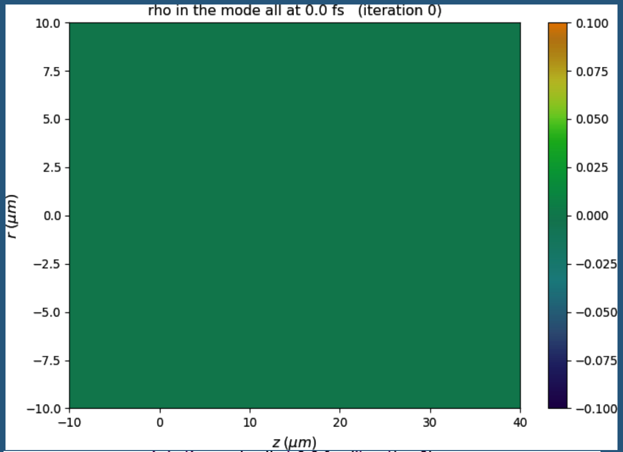

Spatial charge ($C/m^{3)}$)

Starting Position

0 fs

0 μm

0 interactions

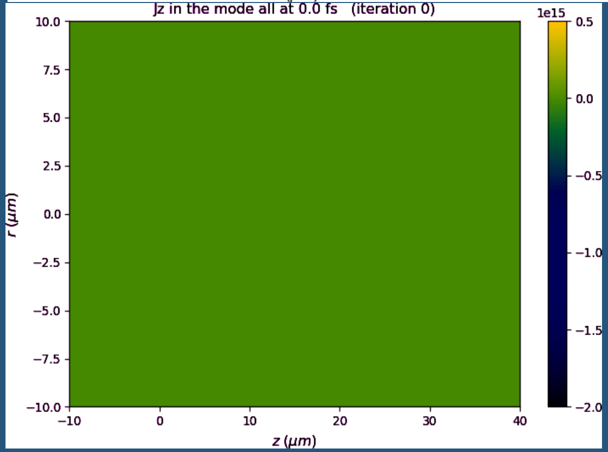

Current density

(A/ m^2)

25.7 fs

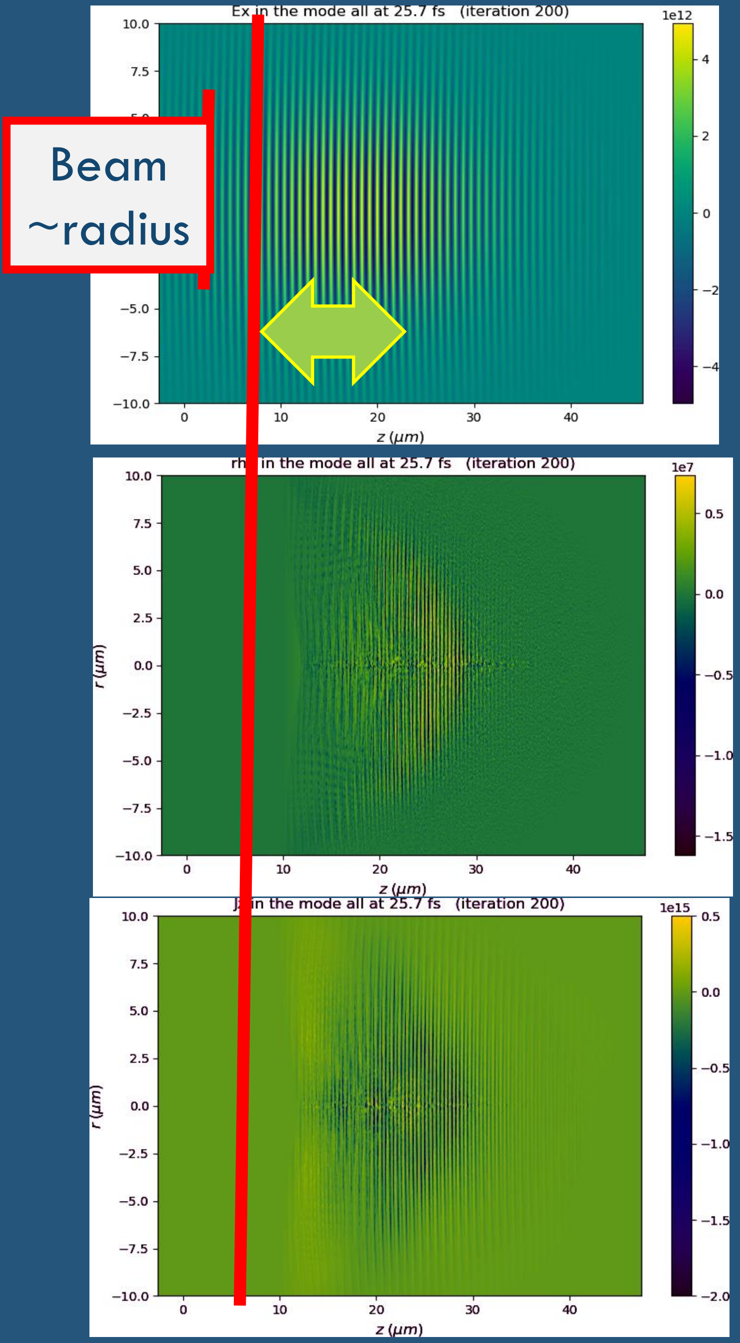

λ

And

λ_p

51.3 fs

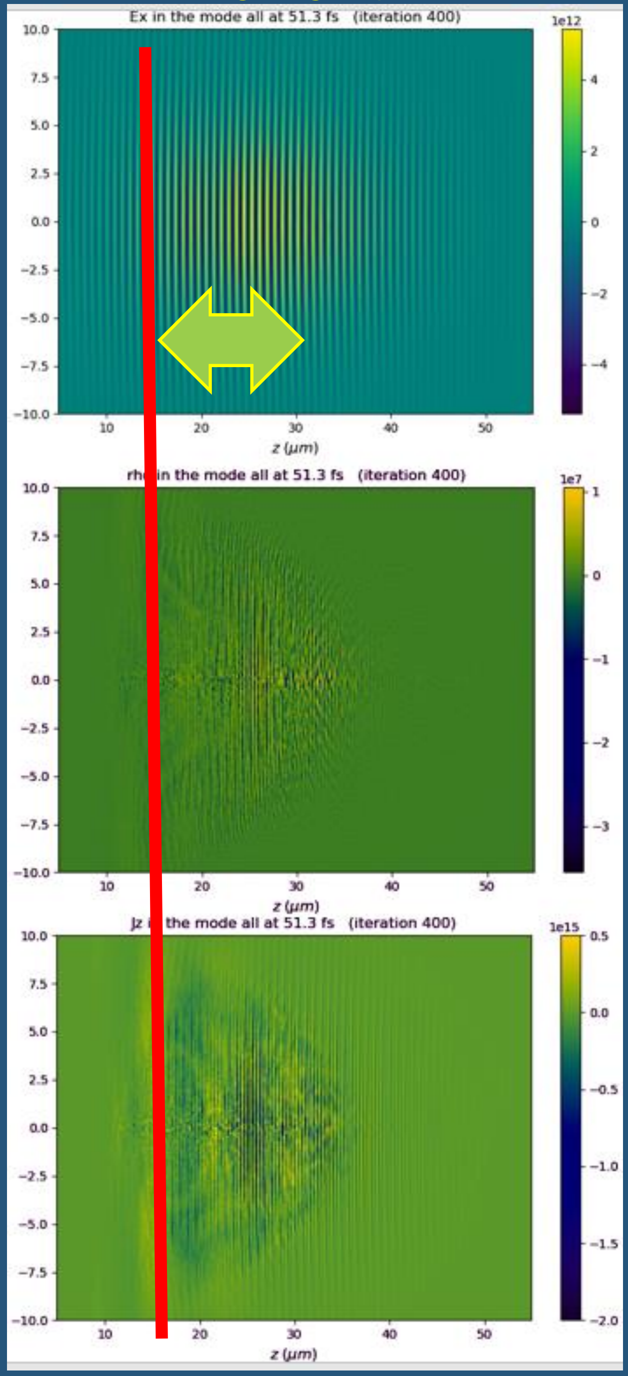

77.0 fs

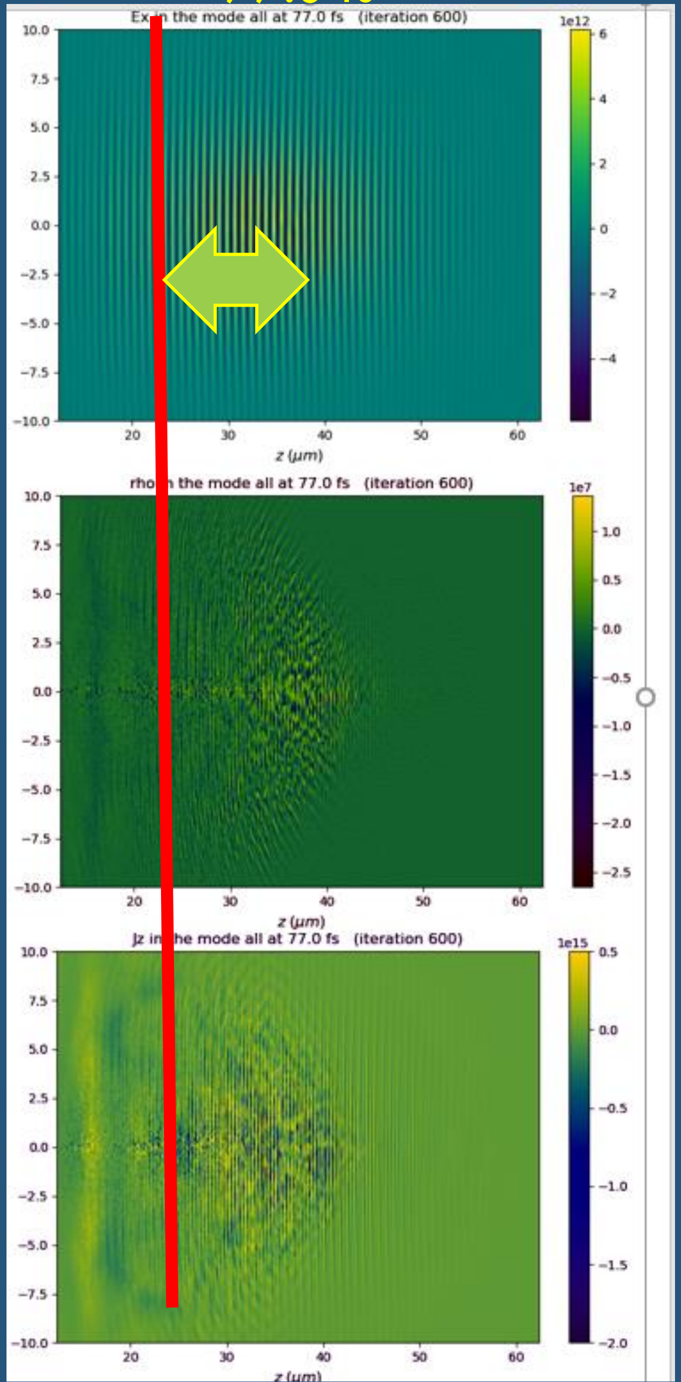

Self focusing

154 fs

205 fs

307 fs

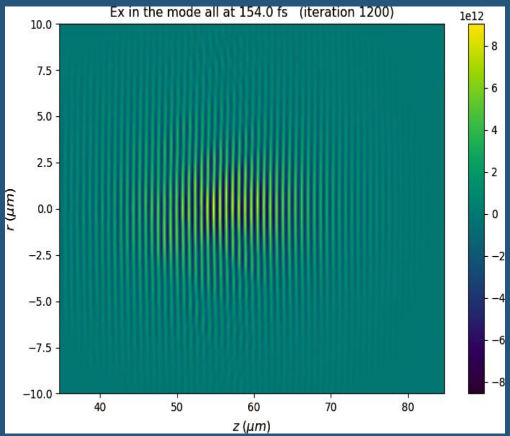

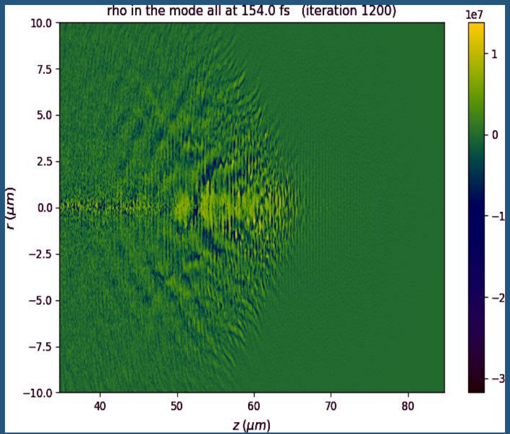

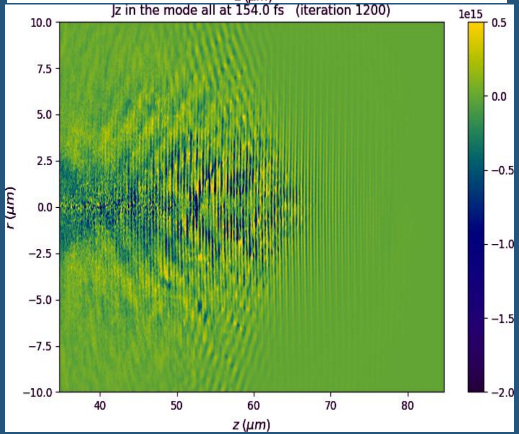

Beam ~radius

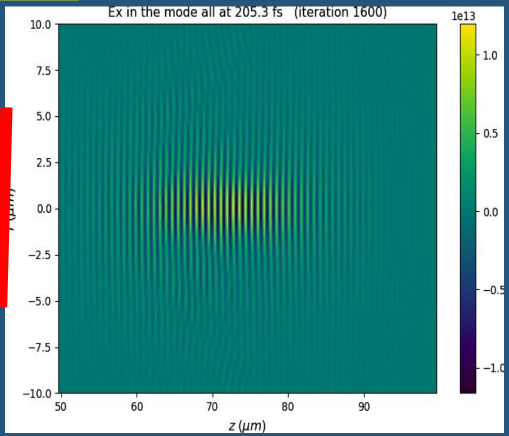

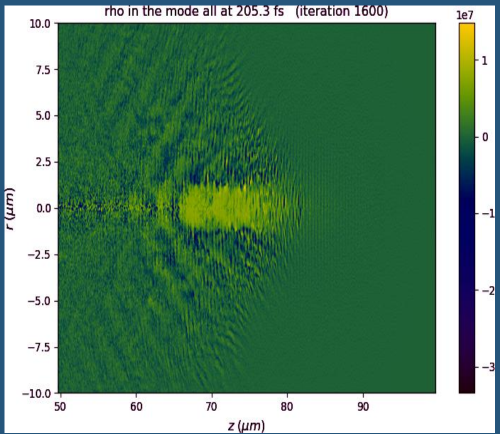

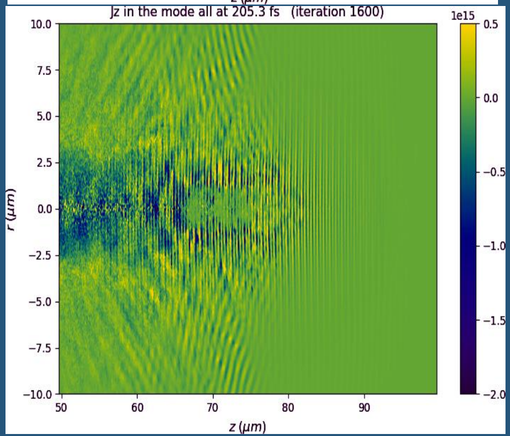

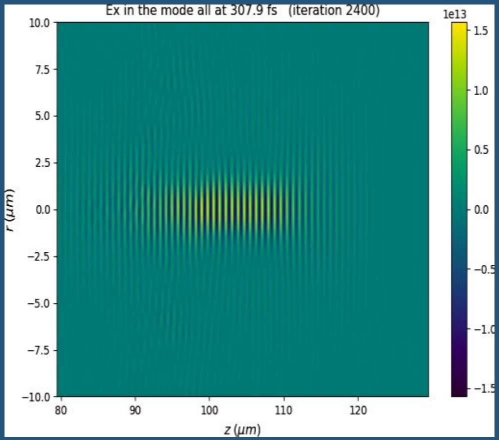

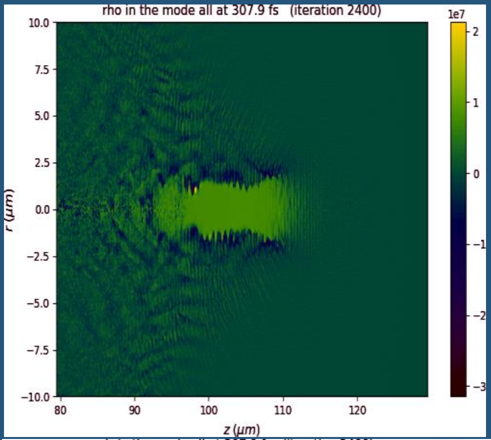

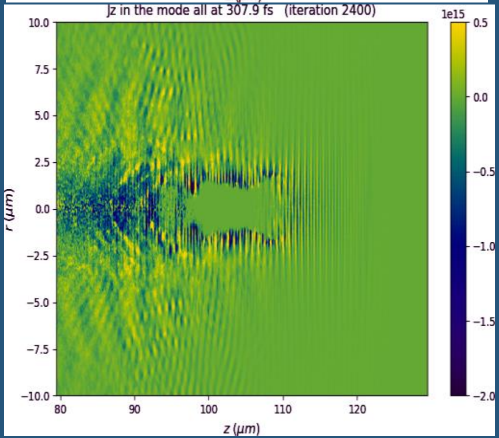

359 fs

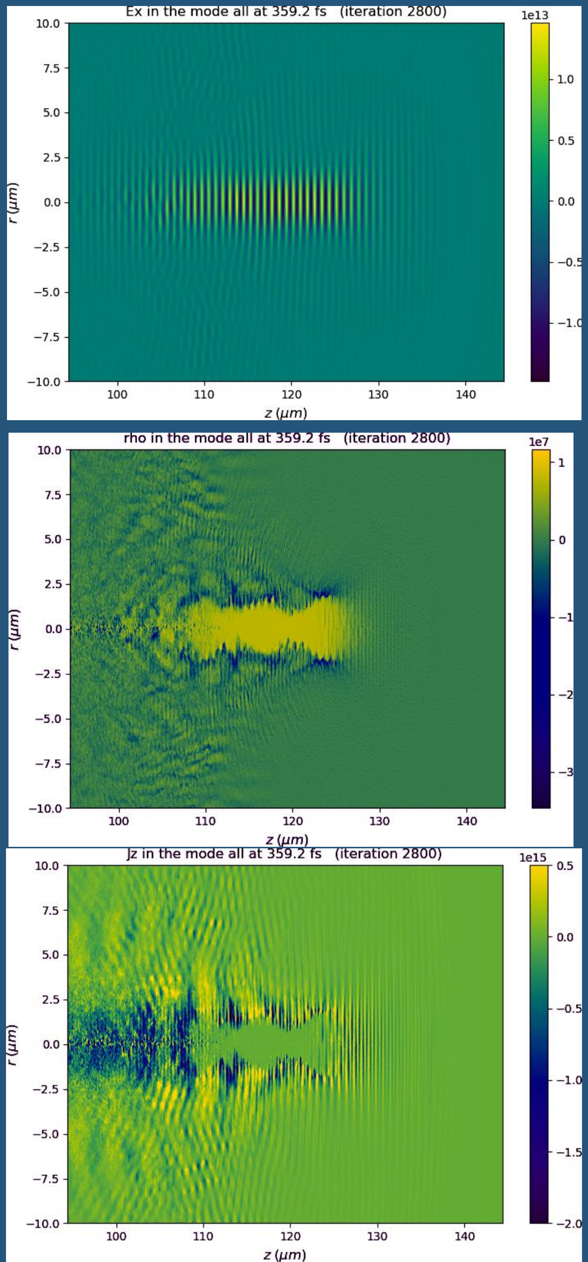

410 fs

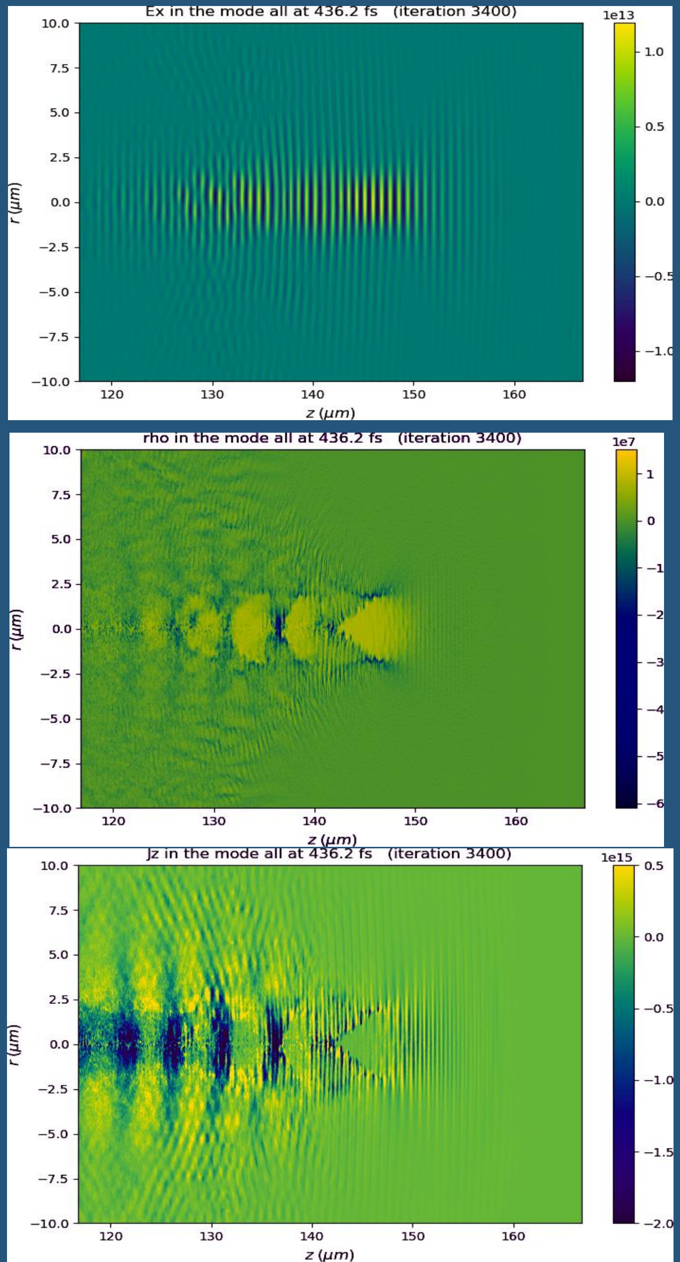

487 fs

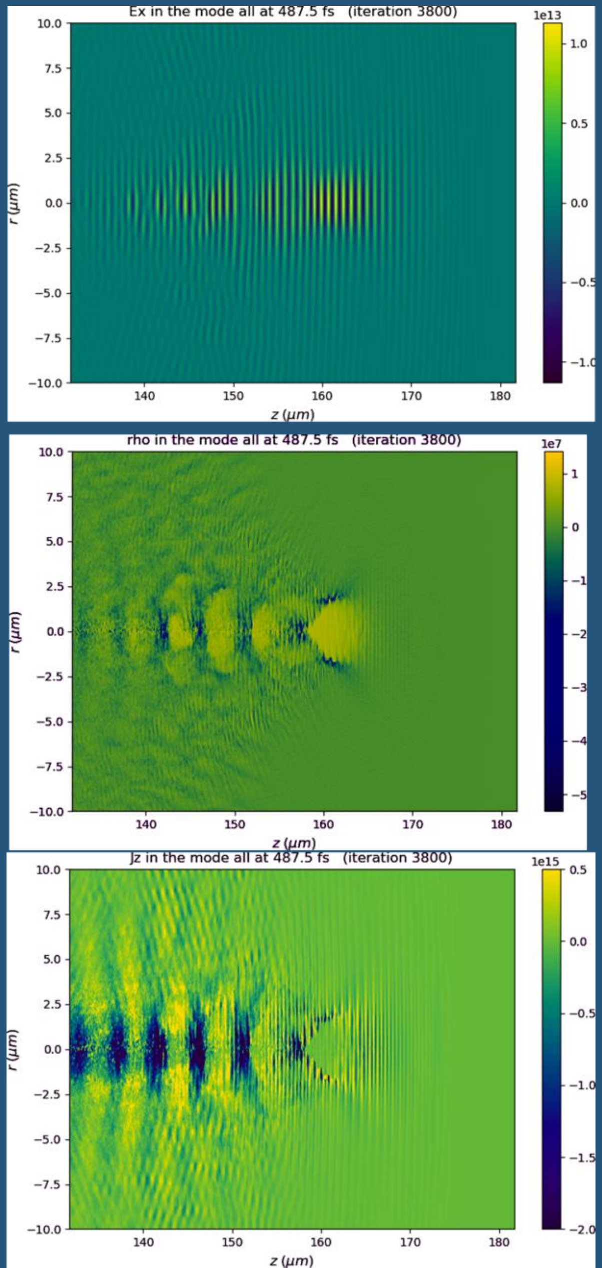

515 fs

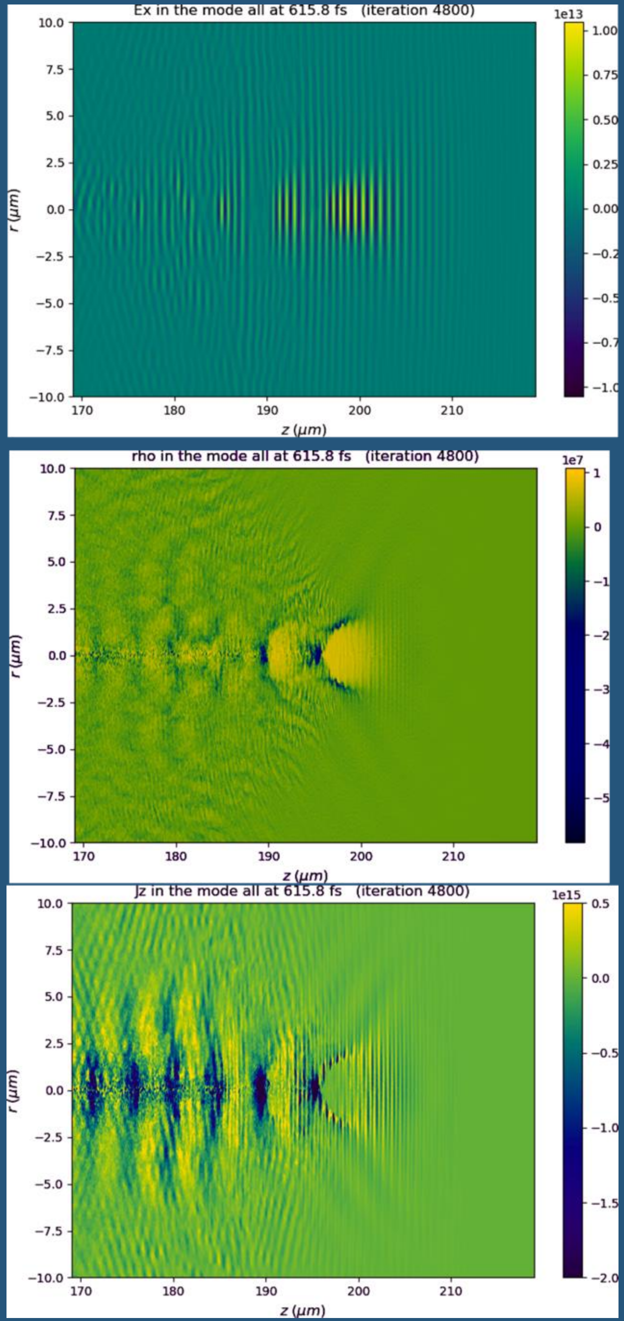

692 fs

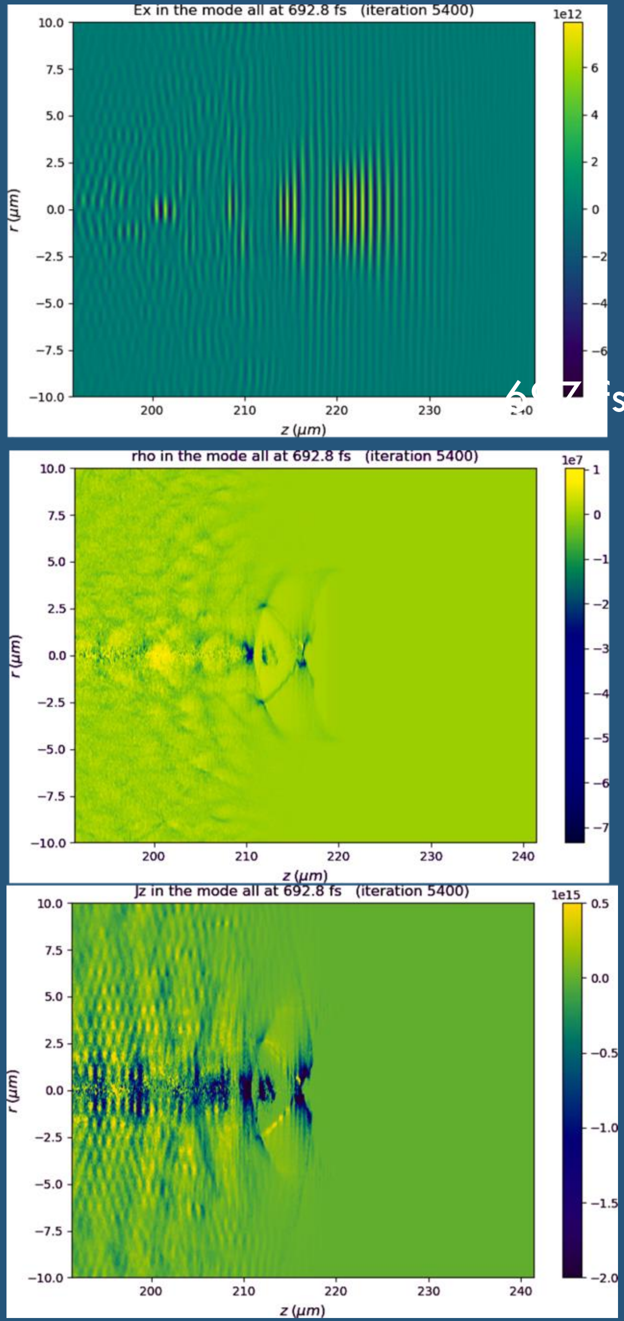

769 fs

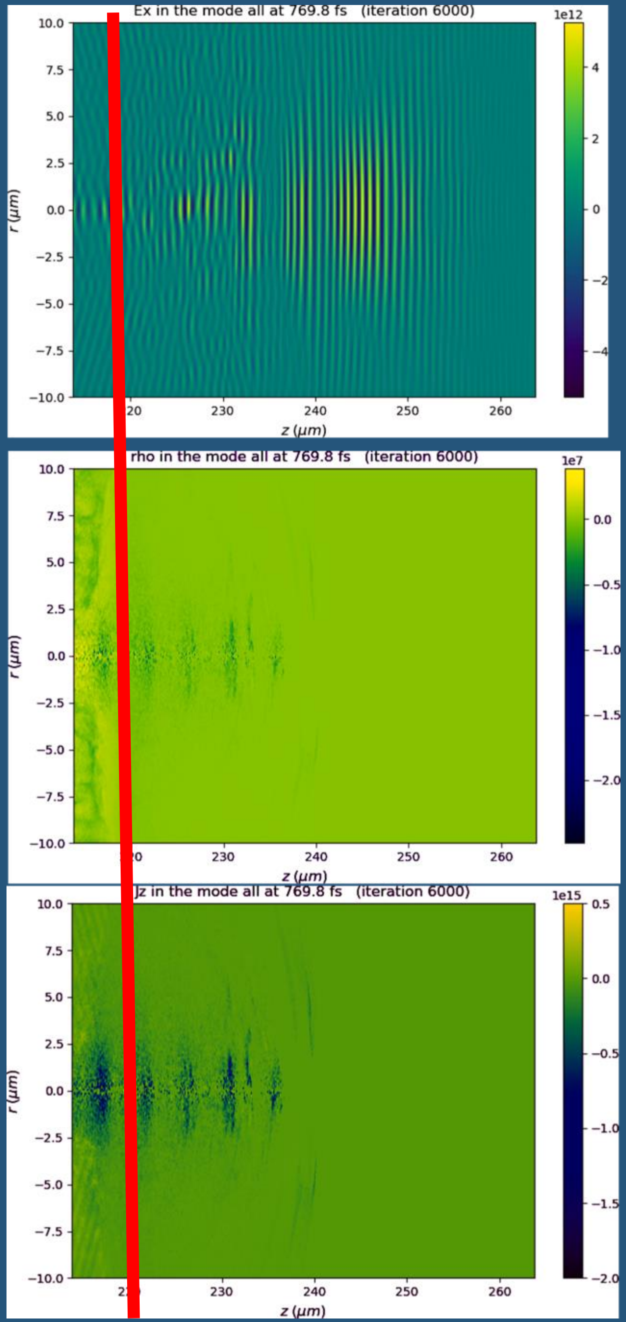

RESULTS OF SIMULATION

- 4 TW is enough for produciton of a 4 MeV electron beam with great divergence, nC charge,
- series of bunches, with fs duration
- Electron Injection is due to the self focuuing and acceleration occurs in the self modulated regime.

PROTON ACCELERATION – TNSA MODEL
THE ELECTRONS CLOUD ATTRACTS THE PROTONS

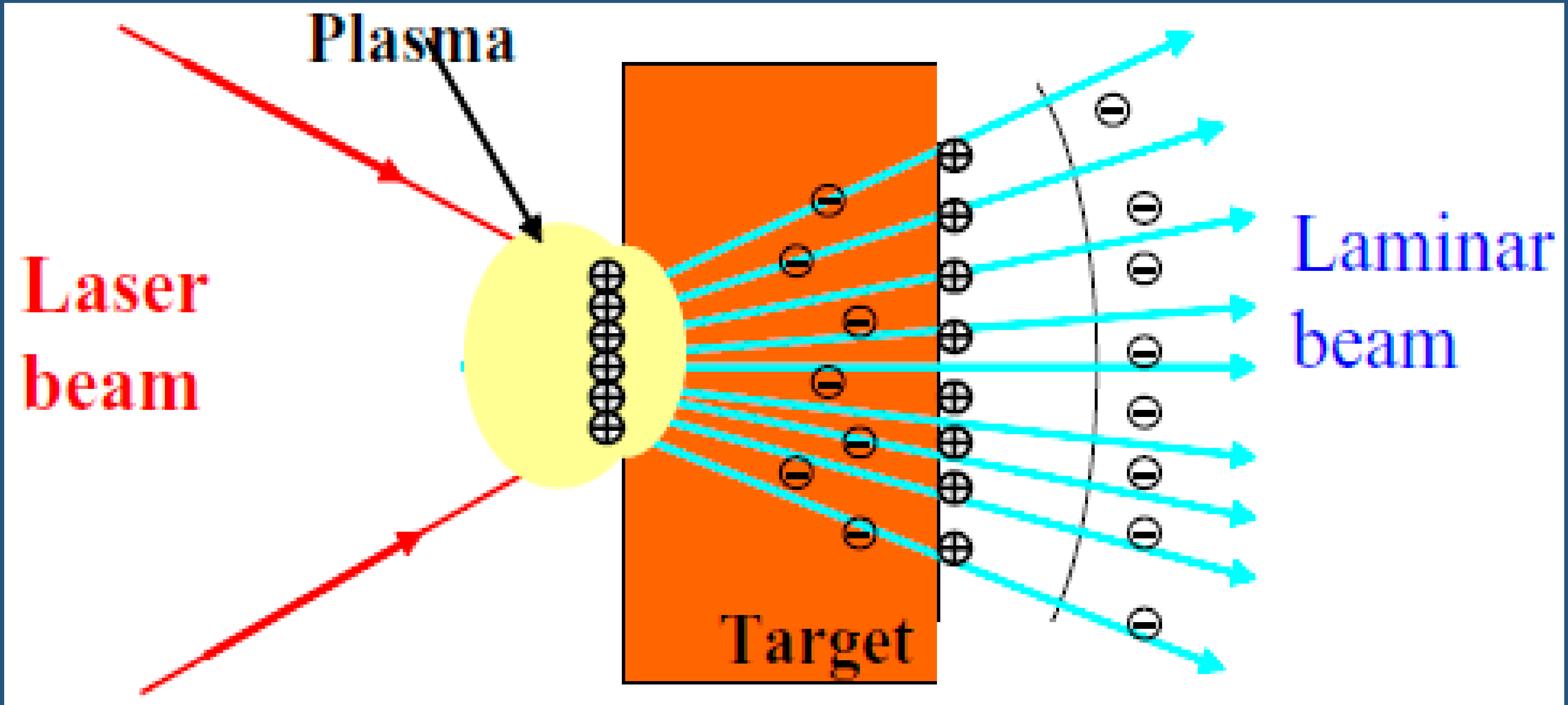

- Ion Acceleration—Target Normal Sheath Acceleration, M. Roth and M. Schollmeier, e Proceedings of the CAS-CERN Accelerator School: Plasma Wake Acceleration, Geneva, Switzerland, 23–29 November 2014

PROTON ENERGY x LASER INTENSITIES

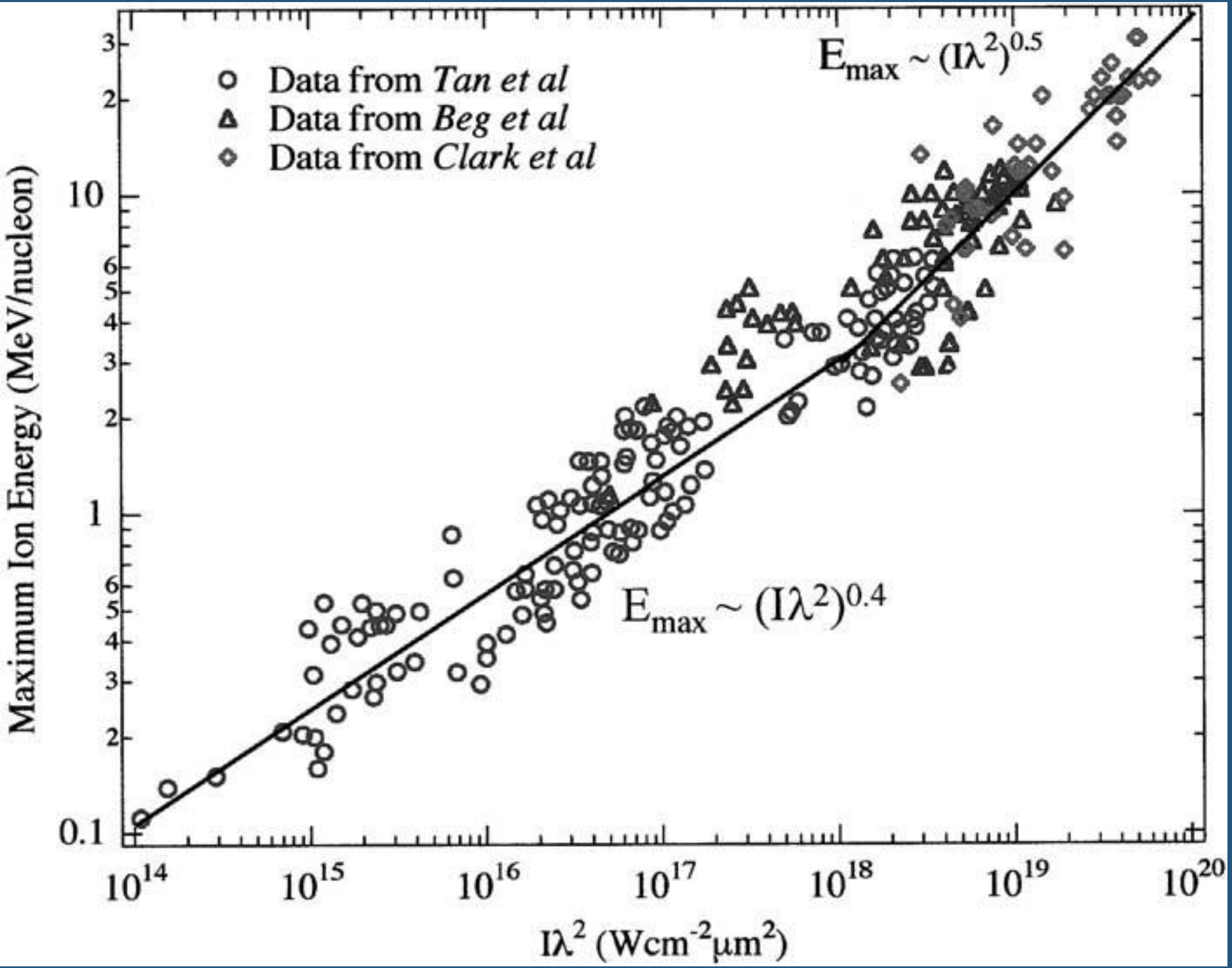

100 MeV
Vulcan, RAL

TABLE TOP NUCLEAR REACTIONS (ONLY FEW MEV)

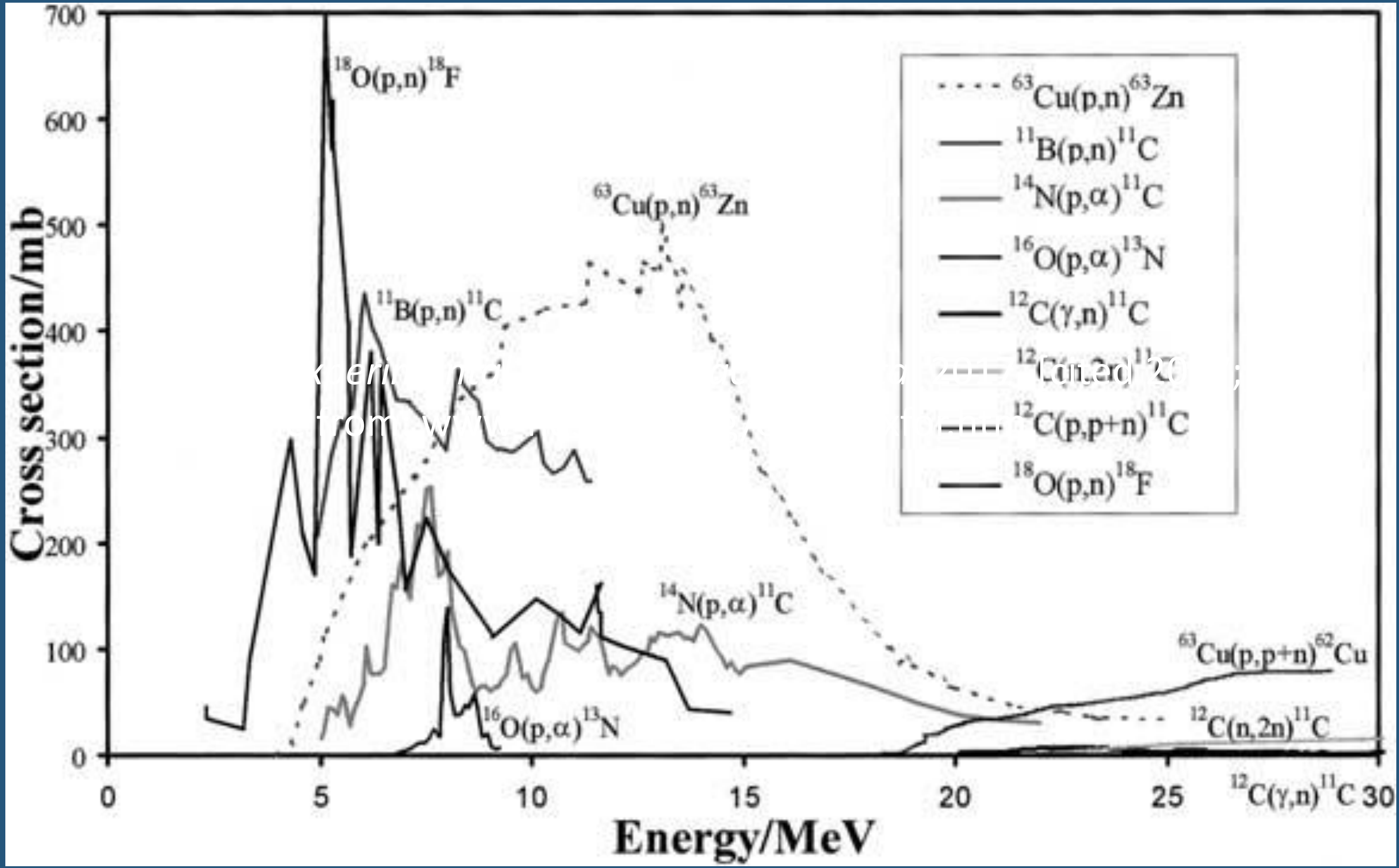

EXFOR: Experimental Nuclear Reaction Data. 2017 [cited 2017; Available from: www-nds.iaea.org/exfor/exfor.htm

PROTON THERAPY –BRAGG PEAK

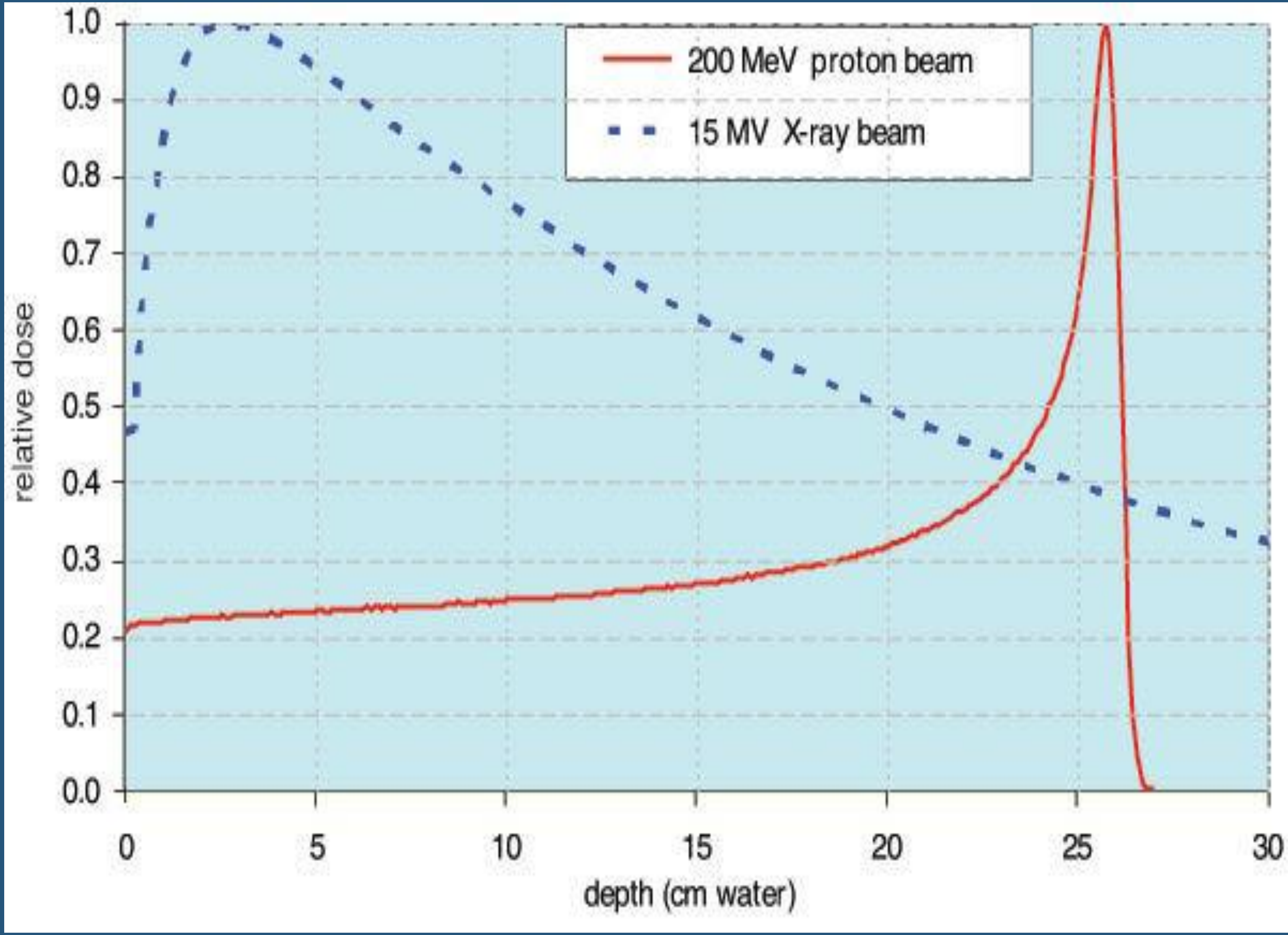

Protonteraphy

Due to the high resolution and depth:
needs a strategic therapeutic plan to treat the tumor

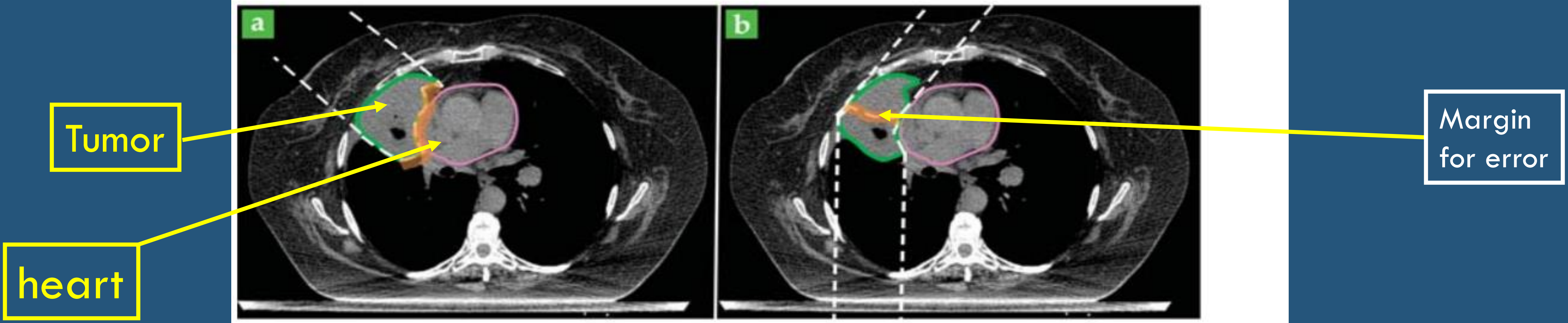

Figure 1. For a lung tumor (outlined in green) abutting the heart (pink), the ideal treatment plan **(a)** would use a single proton beam (outlined by dashed white lines) that stops at the deepest edge of the tumor. Due to the beam-range uncertainty, however, a margin (orange shaded area) must be added to the treatment area targeted for the full prescribed radiation dose. The end of the beam range is thus inside the heart, which may suffer severe damage or functional complications. To avoid such risk to critical organs, a suboptimal plan **(b)** with two beams might be used instead, even though it now delivers a low to intermediate radiation dose to the healthy lung.

Physics Today 68, 10, 28(2015); https://doi.org/10.1063/PT.3.2945

62 (+38) Proton Therapy Facilities around the world

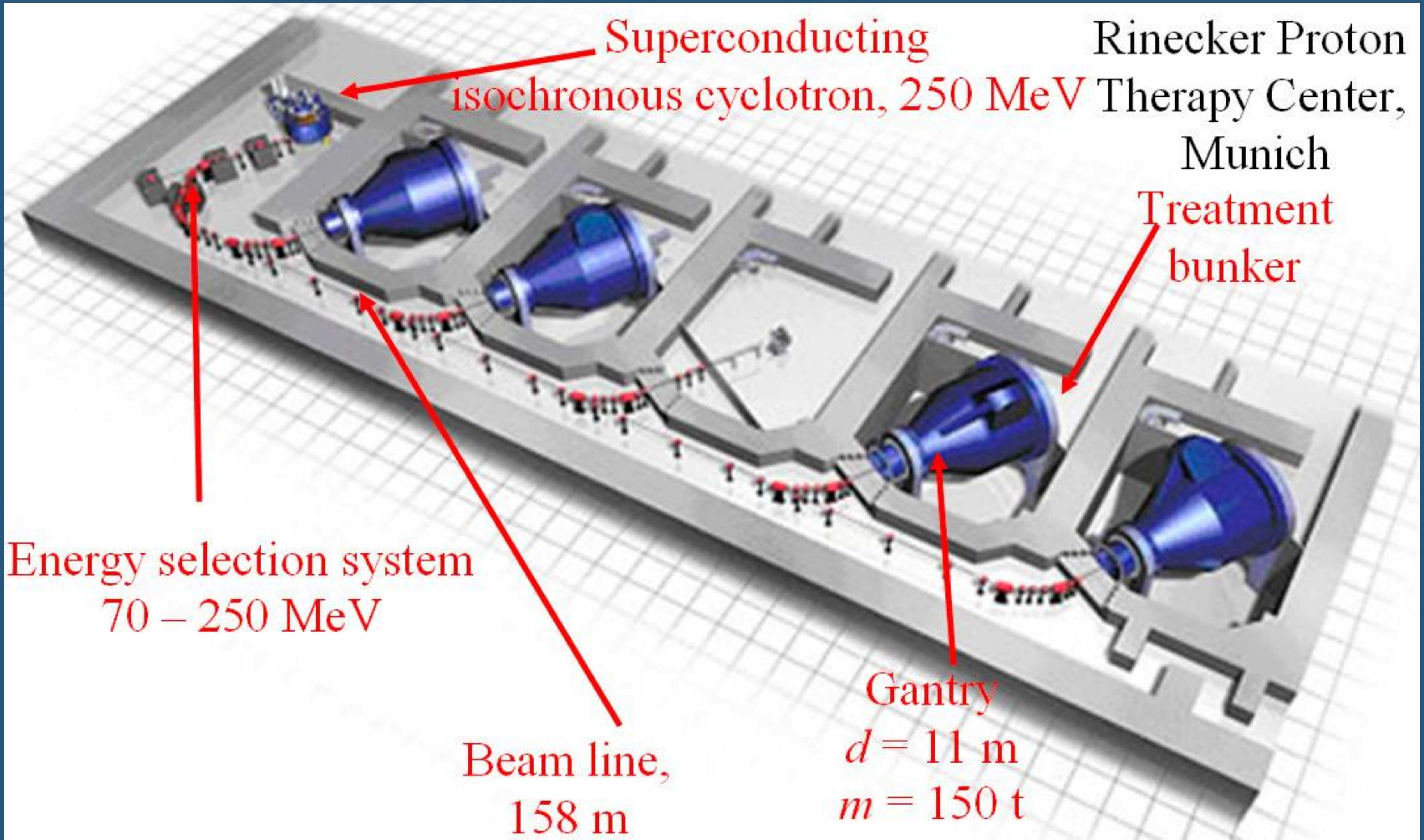

Actual Cost:
US$ 200,000,000

Predicted Cost
With Laser:
US$ 20,000,000

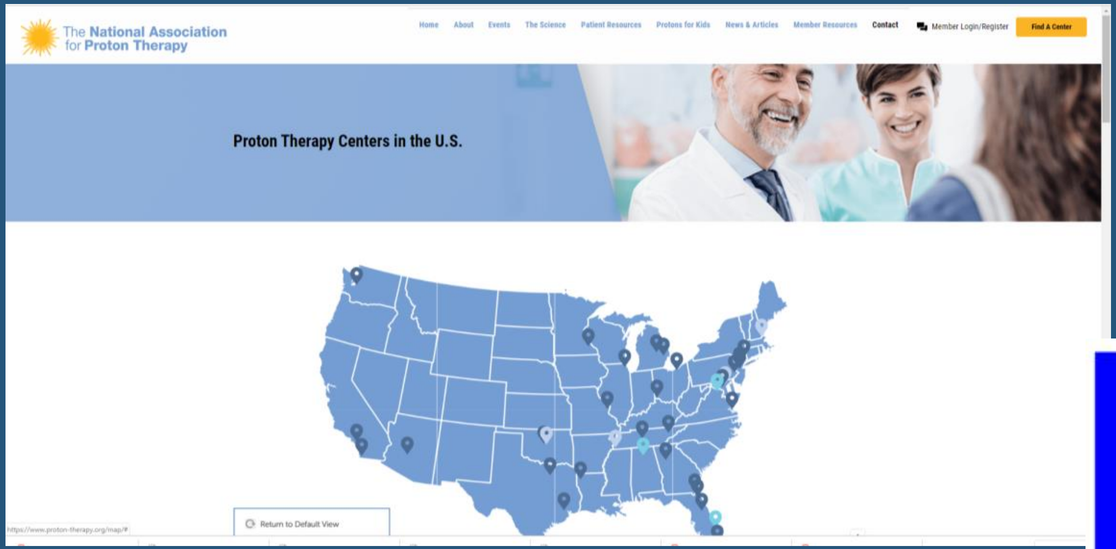

28 + 4 under construction

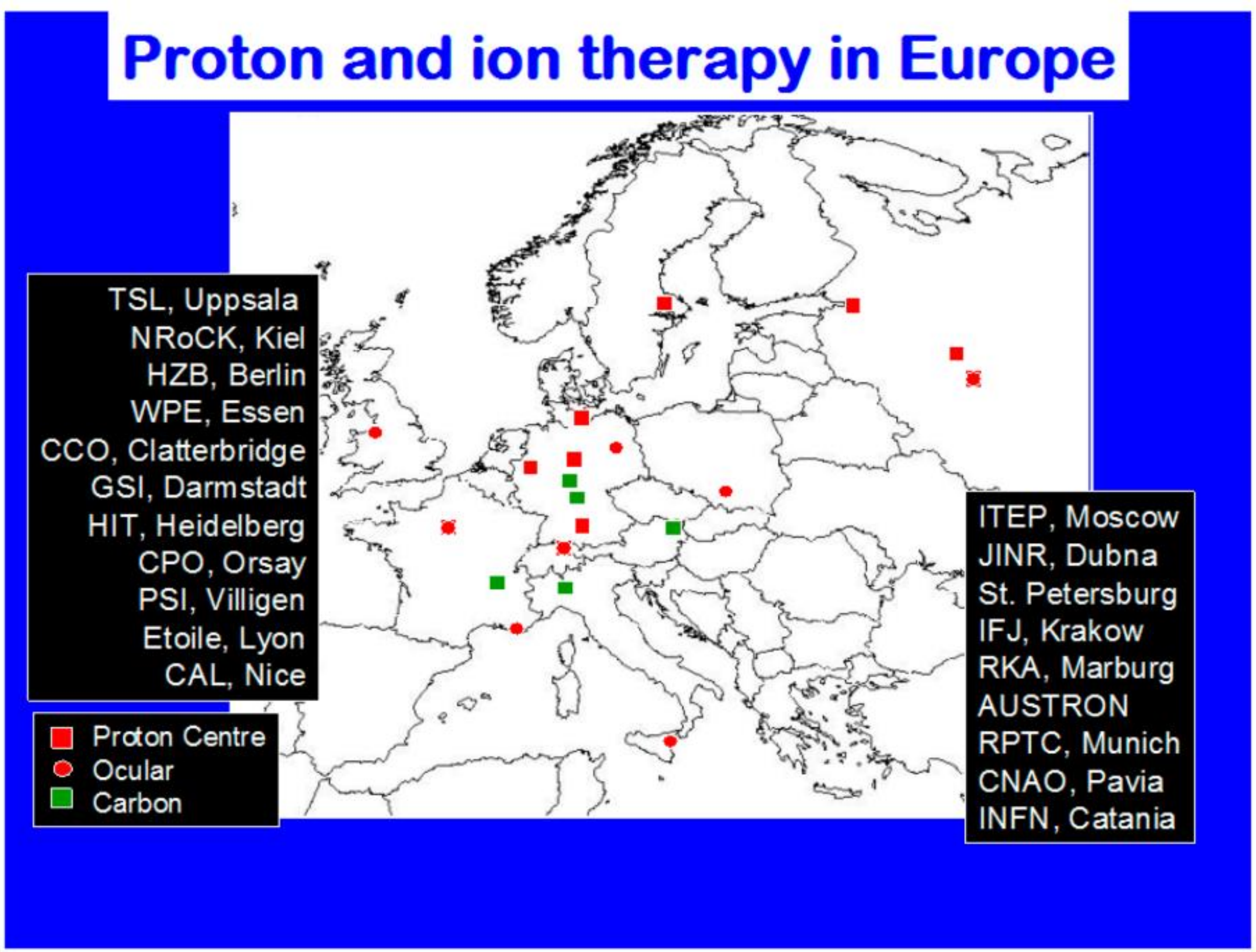

PROTON THERAPY FACILITIES IN CLINICAL OPERATION

(LAST UPDATE: SEP 2019) HTTPS://WWW.PTCOG.CH/INDEX.PHP/FACILITIES-IN-OPERATION

Country	Energy(MeV)	Starting year
Austria	250	2015
Canada	72	1995
Czech Republic	230	
China (2)	250	2004, 2014
Denmark	250	2015
England (3)	62, 230, 250	1989, 2018, 2018
France (3)	65, 230, 230	1991, 1991, 2018
Germany (6)	250 (5), 430	1998, 2009, 2012, 2013. 2015
India	230	2019
Italy (3)	60, 230, 250	2002, 2011, 2014
Japan (14), mostly Synchrotron	220 - 250	1994 -2018
Poland	230	2011
Russia (4)	200-150	1969-2018
South Africa	200	1993
South Korea (2)	230	2007-2015
Switzerland	250	1984
Taiwan	230	201'5
The Netherlands (3)	230-250	2018
USA (13)	230-250	1990- 2014, 4 under construction
Total	62 (+ 38 under construction)	

35 LASER FACILITIES: ACCELERATION FOR MEDICAL PURPOSES

[HTTPS://WWW.PTCOG.CH/INDEX.PHP/FACILITIES-IN-OPERATION](https://www.ptcog.ch/index.php/facilities-in-operation)

- PW Vulcan at RALab is now 40 y.o.
- ELI europe
- LaserNetUS
- 4 PW laser in China
- 100PW laser in Russia

CUOS, University of Michigan	Ultra short pulsed laser	Ti:Sapphire	10TW, 100fs
Principle method	Interaction between high electric field and matter		
Research topics	High field physics Medical application (eye surgery)		
Max Born Institute			100TW, 35fs, 10Hz
Principle method	Interaction between high electric field and matter		
Research topics	High field physics Automobile processing		
ASTRA, Rutherford Appleton Laboratory			40fs, 500mJ
Principle method	Interaction between high electric field and matter		
Research topics	Detection of explosive, Tightening molecular binding, High speed processing in molecular ions		
LOA			~PW
Principle method	Interaction between high electric field and matter		
Research topics	Medical application, PET, High field physics		
INRS, Universite du Quebec			2TW, 500fs and 10TW, 60fs
Principle method	Interaction between high electric field and matter		
Research topics	Laser plasma interaction		
RRCAT, Indore	-	-	100TW + 7TW, 25-40 fs, Ti-sapphire
Principle method	Interaction of intense light with matter		
Research topics	X-ray emission, x-ray applications		
TIFR, Mumbai			100TW + 20TW, 25-40 fs, Ti-sapphire
Principle method	Interaction of intense light with matter		
Research topics	X-ray emission, giant magnetic fields, cluster ionization		
Politecnico di Milano			<10fs, wavelength tunable
Principle method	Ultara short pulse generation, Parametric amplification, Pulse compression with hollow fiber		
Research topics	High speed spectroscopy of molecular system, At-second coherent x ray generation, Laser material processing		
Shanghai institute of optics and fine mechanics			23TW, 33.9fs
Principle method	Optical parametric chirped pulse amplification		
Research topics	Quantum optics, High intensity high speed laser physics		
[illegible]			5fs
Principle method	Pulse compression with gas capillary		
Research topics	High order harmonics generation in water window region, x-ray microscopy		
University of Vienna			~ Atseccond
Research topics	Quantum control, time resolved material observation, control, laser chemistry		
LULI		Nd:glass	Sub-picosecond, 100TW
Principle method	Interaction between high electric field and matter		
Research topics	Astronomy Terrestrial physics		
Jena University		Diode laser	
Research topics	Nuclear transformation		
APRI, GIST	XUV, Coherent X-ray	Ti:sapphire	0.75 J, 25 TW, 30 fs, 10 Hz
Principle method	wakefield acceleration		
Research topics	Laser accelerator		
[illegible]	Ultra-short UV laser	Ce:LLF pumped by KrF	100fs, 305nm
Principle method	Ultra short pulsed laser interaction with matter		
PHELIX, GSI	Heavy ion beam	Ti:Sapphire Nd:glass hybrid	500J, 500fs, 1PW
Principle method	Interaction between heavy ion beam and high power laser		
Research topics	Heavy ion beam interaction with matter		
LLNL	Coherent x ray	X-ray laser	~μJ, 12.1nm
Principle method	Transient collisional excitation		
Research topics	Interference observation		
Max Born Institute			~μJ, 32nm
Principle method	Radiation application		
Research topics			
Paris-Sud University			~μJ, 14nm
Principle method			
Research topics	Plasma interferometer		
Rutherford Appleton Laboratory			7.3nm
Principle method	Electron collisional excitation		
Research topics	Radiation application		
[illegible]			21.2nm
Colorado State University			3.5mW, 46.9nm
Principle method	Discharge excitation		
Research topics	Obserbvation of biological specimen, optical examination		
DESY		X-ray FEL	230MeV, 80nm (target : 6nm)
Principle method	Undulator		
Research topics	Observation of biological specimen, solid state physics, astrophysics		
SLAC			15GeV, 0.1~0.15nm
Principle method	Undulator		
Research topics	Observation of biological specimen, solid state physics, astrophysics		
Argonne National Laboratory			217MeV, 530nm (under upgrading to 700Mev, 51nmj
Principle method	Undulator		
Research topics	To provide high brightness and high temporal resolution synchrotron radiation source		
SPARX, INFN			itarget : 1.5nm in 2007j
[illegible]			itarget : 10nm in 2007 and 1.2nm in 2009j
4GLS, Daresbury Laboratory			600MeV, 12nm~75μm
Research topics	Combination of IR-FEL, VUV-FEL, XUV-FEL, and synchrotron radiation		
CHESS, Cornell University	Ultra short pulsed x-ray	ERL-LS	7GeV, 100mA, 100fs, 1.3GHz
Research topics	X-ray research		
Brookhaven National Laboratory			100fs,106~108 photons/pulse
Principle method	Super conducting linac		
Research topics	High speed structural dynamics, high speed process diagnostics, microscopy, coherent x-ray scattering, structural biologu		
LBL			10-100fs, 10kHz, 1-10keV
Research topics	High speed x-ray science, pump and probe experiment		
ERLSYN, Erlangen University			3.5GeV, 200mA, 1.6mrad, 100fs
Research topics	Chemistry, biology, crystallography, material science		
Jefferson Laboratory	NIR and UV	ERL-FEL	10kW
Research topics	Photo nuclear reaction, material control, non-thermal processing		
BINP			(20MeV ERL)
Duke University	ƒÁ ray (~250MeV)	FEL	1GeV, 193~400nm
Principle method	Inverse Compton scattering		
Research topics	Photo nuclear reaction, solid state physics		

Financial Support - Phase 1, 2017-2020

- FAPESP Week (Nebraska &Texas-2017);
- Visiting Scientist 2017/21124-0;
- Project: Mobility-University of Nebraska-Lincoln (2018/2596
- FAPESP Institutes 2017/50332-0;
- Project CNPq 300616/2017-1
- Project (N° 63230.004277/2018-55)
- Submitted: FAPESP-FAPERG 2019/15387-4
- FAPESP Pos-doctoral position in the project

Map of the High intensity Lasers > 1 x 10^{19} W/cm^2

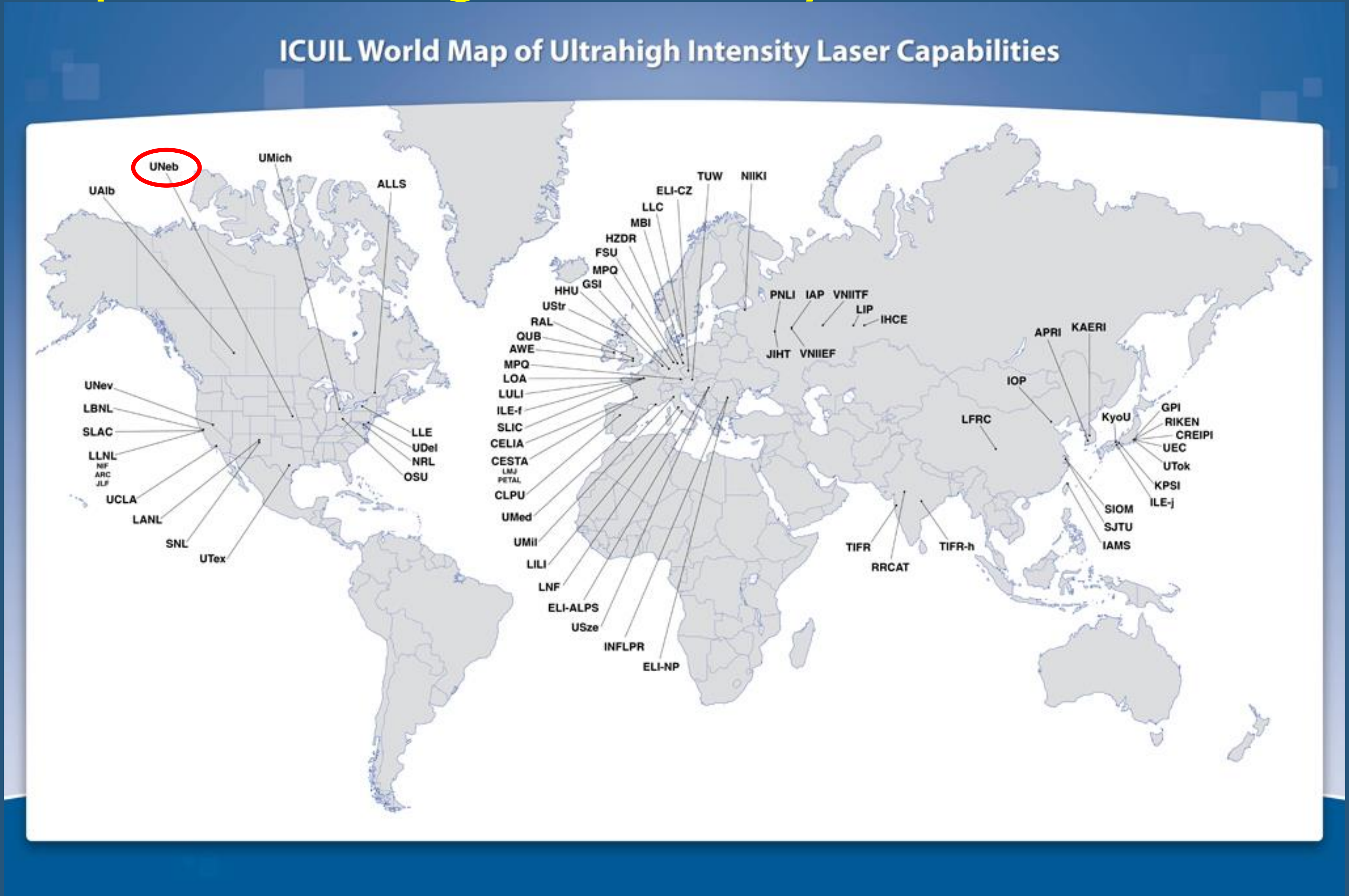

THANK YOU FOR YOUR ATTENTION